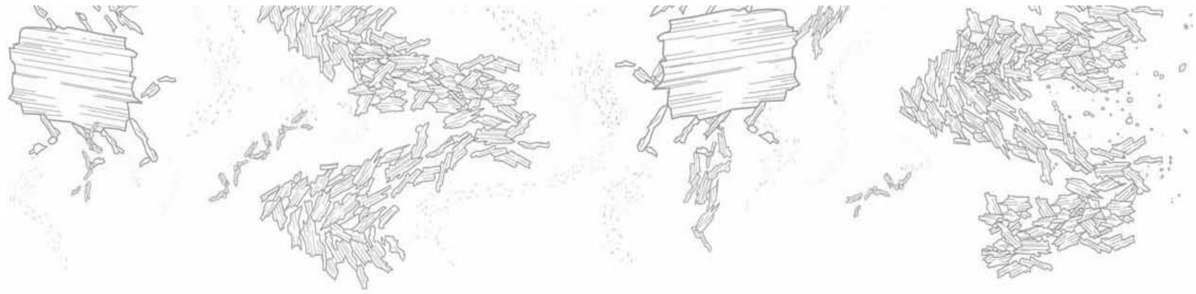

Metamorphic Reactions

Questions to be Considered in this Chapter:

1. What advantages are gained when we consider changes in mineral parageneses (such as isograds) as reactions?
2. What various types of reactions occur in metamorphic rocks, and what principal intensive variables control the progress of each?
3. What are the effects of variable fluid and mineral compositions on the grade and temperature interval over which a reaction takes place?
4. How can we deal with multiple reactions represented on a single phase diagram, such as a pressure–temperature diagram? What happens when some reactions have several phases in common, and their intersection reduces phase rule variance?
5. In what ways might actual reaction processes differ from the reactions as typically written?

Although metamorphism may involve a number of changes, including recrystallization of preexisting phases and diffusion, the most dramatic and useful changes involve metamorphic reactions that generate new mineral phases or modify the composition of existing ones. In this chapter, we address mineral changes that involve reactions.

The classic notion of an **isograd** is that it is a line in the field that demarcates the first appearance of a new mineral phase as one progresses up metamorphic grade. Such an isograd is useful in the field because a worker need only be able to recognize new minerals in a hand specimen. More recently, we have recognized that an isograd can also demarcate the *disappearance* of a mineral as grade increases. Such isograds are commonly called **mineral-out** isograds (e.g., "muscovite-out" isograd, Reaction (5)), to distinguish them from the traditional (**mineral-in**) isograds. If the "in" or "out" is not stated, an isograd is accepted to be a traditional mineral-in type.

When we realize that reactions are always responsible for introducing or consuming mineral phases during metamorphism, we gain considerably in our understanding of metamorphic processes and isograds. If we treat isograds as *reactions*, we can then understand what physical and/or chemical variables affect the location of a particular isograd. Some investigators have advocated that we distinguish simple field-based mineral-in and mineral-out isograds (without a specified reaction) from reaction-based isograds. Miyashiro (1994), for example, referred to simple isograds as "tentative isograds," implying that more detailed petrographic and laboratory work on rocks below, at, and above the isograd would reveal the nature of the reaction responsible. Although every isograd must represent some sort of reaction, the exact reaction is not determined in every case, so many isograds are still characterized by, and named for, the index mineral for which they mark the appearance or disappearance.

A student may wonder why, after over a century of research in metamorphic terranes, we can't simply look up which reaction is responsible for the introduction of any particular mineral. The problem is that more than one reaction can produce any single mineral. In 10 minutes of searching my office bookshelf, I found 23 reactions that could produce biotite as one of the reaction products. I'm sure there are many more. Some of the reactions were prograde and others retrograde. Because biotite occurs in a variety of igneous rocks as well, we also know that it can be generated by reactions involving the crystallization of melts. Which reaction is responsible for the "biotite isograd" depends upon the minerals present below the isograd (the potential reactants), which, in turn, are determined by the rock composition and the metamorphic grade (*P* and *T*). Care must therefore be exercised when addressing isograds based simply on the appearance or disappearance of a mineral, and an attempt should always be made to determine the responsible reaction or reactions.

If we understand the nature of the reactions that produce metamorphic minerals, the physical conditions under which any particular reaction occurs, and what physical variables affect a reaction and how, we can use this knowledge to understand metamorphic processes better. If we have good experimental and thermodynamic data on minerals and reactions we can locate a reaction in *P-T-X* space and constrain the conditions under which a particular metamorphic rock formed. In this chapter we will review the various types of metamorphic reactions and discuss what affects them and how.

1 POLYMORPHIC TRANSFORMATIONS

Single-component polymorphic transformations, such as among the polymorphs of SiO_2 or Al_2SiO_5, graphite–diamond, or calcite– aragonite, etc. are in many ways the simplest to deal with. Because the alternative phases are of essentially fixed and identical composition, the transformations depend on temperature and pressure only and are minimally affected by variations in the composition of the system in which one or another polymorph is found. For example, as long as pure $CaCO_3$ is stable in a rock system, it should occur as calcite at pressures below the equilibrium curve in Figure 1, and as aragonite at pressures above the curve. This explains why aragonite is the stable $CaCO_3$ polymorph typically found in blueschist facies terranes. Similar arguments hold for essentially all polymorphic transformations, and, provided that the boundary curves have been located accurately by experiments and that the mineralogy reflects equilibrium conditions, the presence of one or another polymorph may conveniently be used to set limits on the temperature and pressure conditions under which a rock formed. For example, we can use the presence of andalusite to indicate low-pressure metamorphic conditions, and we can effectively limit the pressure of andalusite-bearing rocks to values below ~0.38 GPa.

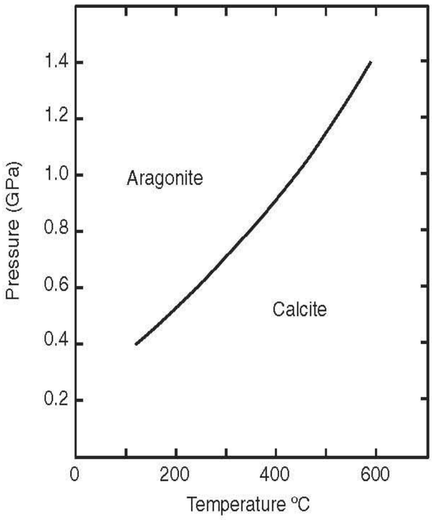

FIGURE 1 A portion of the equilibrium boundary for the calcite–aragonite phase transformation in the $CaCO_3$ system. After Johannes and Puhan (1971). Copyright © with permission from Springer-Verlag.

The presence of two coexisting polymorphs in a single rock has generally been taken to indicate that the metamorphic peak corresponded to equilibrium conditions along the univariant boundary curve separating the pair. If an independent estimate of either pressure or temperature is available, the other parameter may then be estimated from the location of the equilibrium curve. For example, if kyanite and sillimanite were to be observed together, and the pressure were estimated via geobarometry to be 0.5 GPa, then the temperature of equilibration could be determined to be approximately 560°C. *If* all three Al_2SiO_5 polymorphs were to be found in *stable* coexistence, the assemblage would indicate conditions at the invariant point (ca. 500°C and 0.38 GPa).

Because of the small changes in entropy and volume for most polymorphic transformations, the difference in Gibbs free energy between two alternative polymorphs may be small, even at temperatures or pressures relatively far from the equilibrium boundary. There is thus little driving force for the reaction to proceed, and crystals of one polymorph may remain as *metastable* relics in the stability field of another. Coexisting polymorphs may therefore represent non-equilibrium states, reflecting overstepped equilibrium curves or polymetamorphic overprints. By carefully observing the textures, one may be able to distinguish partial replacement and metastable coexistence from true stable equilibrium grain boundaries. For example, Hietanen (1956) reported the coexistence of all three Al_2SiO_5 polymorphs in northern Idaho and proposed that the complex sequence of regional and contact events in the area occurred near the invariant point. Others have proposed that kyanite is partially replaced by sillimanite during a prograde event near the kyanite–sillimanite boundary and that andalusite partially replaces kyanite during a later event at lower pressure. See Kerrick (1990) and Kretz (1994) for other examples of coexisting Al_2SiO_5 polymorphs and how they have been interpreted.

Another complication results from (usually minor) variations in the compositions of polymorphs from the pure phases. For example, several authors have noted the presence of Fe^{3+} in some Al_2SiO_5 polymorphs, and microprobe analyses indicate that andalusite tends to admit about twice as much Fe_2O_3 (up to ~2.6 wt.%) as either kyanite or sillimanite (Kerrick, 1990). If we consider this in light of Le Châtelier's Principle, the addition of Fe^{3+} to the Al_2SiO_5 system in which andalusite and sillimanite, for example, were at equilibrium would be offset by the formation of extra andalusite. The effect of adding Fe to the system would thus be to enlarge the stability field of andalusite at the expense of the fields of kyanite and sillimanite. The concentrations of most impurities, however, including Fe, are generally considered to be too low to cause a significant displacement in the position of the equilibrium curves separating the Al_2SiO_5 polymorphs in Figure 21.9. Even in a few cases in which hematite is abundant, Kretz (1994) calculated that the shift in the andalusite–sillimanite equilibrium curve caused by Fe^{3+} would be on the order of 30°C, which is too small to account for the broad andalusite → sillimanite transition observed in some field areas. The coexistence of andalusite and sillimanite in such cases is commonly attributed to the very low ΔG of the andalusite → sillimanite reaction so that the two phases coexist metastably as the transition is overstepped with rising *T*.

2 EXSOLUTION REACTIONS

Exsolution reactions occur in solid-solution mineral series when a **solvus** is encountered, typically upon cooling or decompression. The process involves the unmixing of the solid solution within the composition range covered by the solvus. Typical examples include the alkali feldspar solvus, the peristerite gap in Na-rich plagioclase, and the orthopyroxene–clinopyroxene and calcite–dolomite solvi. Exsolution need not involve minerals of the same family. For example, high-pressure pyroxenes in deep-seated high-grade rocks may dissolve quite a bit of Al_2O_3. When uplifted, the Al-rich pyroxenes may exsolve garnet or plagioclase. Exsolution may result in the development of crystallographically oriented rods or lamellae in the exsolving host or, if diffusion is favorable, distinct separate grains.

3 SOLID–SOLID NET-TRANSFER REACTIONS

Solid–solid net-transfer reactions involve solids only and differ from polymorphic transformations in that they involve solids of different composition. Matter must therefore be transferred from one site in the rock to another in order for the reaction to proceed. The four "general" steps involved in metamorphic reactions characterize this type of reaction. Net-transfer reactions differ from solid–solid ion exchange reactions (Section 6) in that progress of net-transfer reactions results in a change in the modal amounts of the phases involved. Several examples were encountered in the previous chapter, including:

$$\underset{\text{Jd}}{\text{NaAlSi}_2\text{O}_6} + \underset{\text{Qtz}}{\text{SiO}_2} = \underset{\text{Ab}}{\text{NaAlSi}_3\text{O}_8} \qquad (1)$$

$$\underset{\text{En}}{\text{MgSiO}_3} + \underset{\text{An}}{\text{CaAl}_2\text{Si}_2\text{O}_8} = \underset{\text{Di}}{\text{CaMgSi}_2\text{O}_6} + \underset{\text{Sil}}{\text{Al}_2\text{SiO}_5} \qquad (2)$$

$$\begin{aligned} &\underset{\text{Opx}}{4(\text{Mg,Fe})\text{SiO}_3} + \underset{\text{Plag}}{\text{CaAl}_2\text{Si}_2\text{O}_8} \qquad (3) \\ &\quad = \underset{\text{Grt}}{(\text{Mg,Fe})_3\text{Al}_2\text{Si}_3\text{O}_{12}} + \underset{\text{Cpx}}{\text{Ca(Mg,Fe)Si}_2\text{O}_6} + \underset{\text{Qtz}}{\text{SiO}_2} \end{aligned}$$

When diffusion becomes a limiting factor (generally in rocks with very little pore fluid), the reactions may become arrested, as in corona-forming reactions. Minerals involved in solid–solid reactions may contain some volatiles, but the volatiles are conserved in the reaction so that no fluid is generated or consumed. For example, the reaction:

$$\underset{\text{Tlc}}{\text{Mg}_3\text{Si}_4\text{O}_{10}(\text{OH})_2} + \underset{\text{En}}{4\,\text{MgSiO}_3} = \underset{\text{Ath}}{\text{Mg}_7\text{Si}_8\text{O}_{22}(\text{OH})_2} \qquad (4)$$

involves hydrous phases but conserves H_2O. It may therefore be treated as a solid–solid net-transfer reaction.

When solid–solution is limited, solid–solid net-transfer reactions are **discontinuous** reactions. Discontinuous reactions are univariant and tend to run to completion at a single metamorphic grade (where the *P-T-t* path for which pressure and temperature are related crosses the univariant reaction curve). There is thus an abrupt (discontinuous) change from the reactant assemblage to the product assemblage at the reaction isograd. (The reaction behaves as though invariant in such situations, because P and T are not independent, but constrained by the P-T-t path, so $F = C - \phi + 1$.)

All three types of reactions discussed above are relatively straightforward metamorphic reactions and are subject to variations in pressure and temperature, without complications due to variations in rock or fluid compositions. The presence of reactants versus products has commonly been used, in conjunction with experimental work that constrains the location of the reaction in *P-T-X* space, to set limits on the temperature and pressure conditions of a metamorphic event. When solid-solution is pronounced, net-transfer reactions become **continuous** and subject to compositional effects, which will be discussed in Section 5.

4 DEVOLATILIZATION REACTIONS

Reactions that release or consume volatiles are among the most common reactions in metamorphism. They typically evolve H_2O (dehydration reactions) or CO_2 (decarbonation reactions), but virtually any volatile, including O_2, H_2, CH_4, F, Cl, SO_2, etc. may be involved under appropriate circumstances. The present discussion will concentrate on H_2O-CO_2 volatile systems, but the principles involved may be applied to any reaction releasing volatiles.

Because a volatile species is involved, the reactions are dependent not only upon temperature and pressure but also upon the **partial pressure** of the volatile components. For example, the location on a *P-T* phase diagram of the dehydration reaction:

$$\underset{\text{Ms}}{KAl_2Si_3AlO_{10}(OH)_2} + \underset{\text{Qtz}}{SiO_2} = \underset{\text{Kfs}}{KAlSi_3O_8} + \underset{\text{Al–silicate}}{Al_2SiO_5} + \underset{\text{fluid}}{H_2O} \qquad (5)$$

depends upon the partial pressure of H_2O (p_{H_2O}). This dependence is easily demonstrated by applying Le Châtelier's Principle to the reaction at equilibrium. Reaction (5), incidentally, marks the disappearance of muscovite in typical (quartz-dominant) metapelites and thus represents the muscovite-out isograd. Al_2SiO_5 and K-feldspar are both stable at lower grades (although K-feldspar is rarely encountered for most pelite compositions), so this may not make a good mineral-in isograd.

Figure 2 is a *P-T* phase diagram that shows the equilibrium reaction curve for Reaction (5). The heavy equilibrium curve on the right represents equilibrium between the reactants and products under H_2O-saturated conditions ($p_{H_2O} = P_{\text{lithostatic}}$). This is a common assumption, and the heavy curve represents the typical shape of equilibrium curves for dehydration reactions reported in the literature. The hydrous assemblage is nearly always on the low-temperature side of the curve, and the evolved fluid phase is liberated as temperature increases. The concave upward shape is characteristic of all devolatilization equilibrium curves at low pressure because the slope, as determined by the Clapeyron equation:

$$\frac{dP}{dT} = \frac{\Delta S}{\Delta V}$$

is low at low pressures due to the high volume of the fluid phase but steepens quickly at higher pressures because the fluid is most easily compressed. Thus ΔV decreases much more than ΔS with increasing pressure.

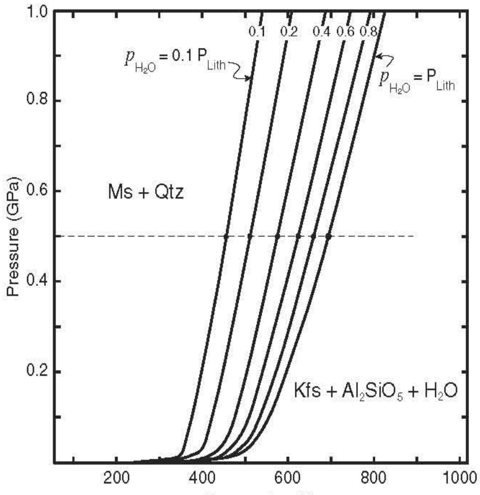

FIGURE 2 *P-T* phase diagram for the reaction Ms + Qtz = Kfs + Al_2SiO_5 + H_2O, showing the shift in equilibrium conditions as pH_2O varies (assuming ideal H_2O-CO_2 mixing). Calculated using the program TWQ by Berman (1988, 1990, 1991).

At very high pressures, the vapor becomes so compressed that many devolatilization curves bend back upon themselves to attain a negative slope. Theoretically, complete devolatilization curves form a closed loop and bend back again at high pressure and low temperature to a positive slope again (Figure 3), but the full loop is rarely, if ever, stable for any reaction. Some greenschist →blueschist reactions, for example, are unusual in that they have the low-*T*/high-*P* portion of the loop stable and are distinguished by having the hydrous phase on the high-temperature side, so that "retrograde dehydration" becomes possible. If we deal only with normal crustal pressures and geothermal gradients, however, devolatilization curves have the shape in Figure 2, and we shall consider this shape to be typical.

Suppose H_2O is withdrawn from the system at some point on the H_2O-saturated equilibrium curve in Figure 2, so that $p_{H_2O} < P_{\text{lithostatic}}$. According to Le Châtelier's Principle, removing H_2O at equilibrium will be compensated by Reaction (5) running to the right, thereby producing more H_2O to compensate for the loss. This stabilizes the right side of the reaction at the expense of the left side. In other words, as H_2O is withdrawn, the Kfs + Al_2SiO_5 + H_2O field expands at the expense of the Ms + Qtz field, and the reaction curve shifts toward lower temperature in Figure 2. I have

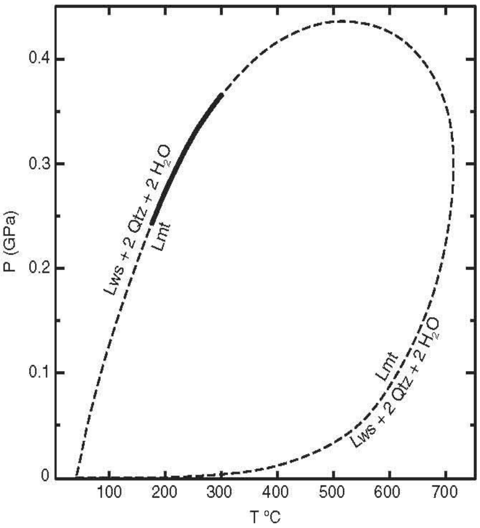

FIGURE 3 Calculated *P-T* equilibrium reaction curve for a dehydration reaction illustrating the full loop that is theoretically possible. Rarely, if ever, is the loop completely stable. In the present case, only the upper portion of the Lmt = Lws + 2 Qtz + H_2O reaction is stable. The experimentally determined equilibrium curve is shown in Figure 19, where the stable section is located between approximately 180 and 300°C at 0.3 GPa (solid portion). Dehydration occurs with *decreasing* temperature for this stable segment of the reaction curve (an unusual situation).

calculated the curve shift for values of p_{H_2O} = 0.8, 0.6, 0.4, 0.2, and 0.1 times P_{lith} and included the curves in the figure.

p_{H_2O} can become less than P_{lith} in either (or both) of two ways. First, P_{fluid} can become less than P_{lith} by simply drying out the rock and reducing the fluid content ($p_{H_2O} = P_{fluid} < P_{lith}$). Second, P_{fluid} can remain equal to P_{lith}, but the H_2O in the fluid can become diluted by adding another fluid component, such as CO_2 or some other volatile phase ($p_{H_2O} < P_{fluid} = P_{lith}$). I calculated the curves in Figure 2 for the latter case, assuming ideal dilution of H_2O at $P_{fluid} = P_{lith}$.

An important point arising from Figure 2 is that *the temperature of an isograd based on a devolatilization reaction is sensitive to the partial pressure of the volatile species involved.* An alternative way to show this is to use a ***T-X*$_{fluid}$ phase diagram** (Greenwood, 1967a). Because H_2O and CO_2 are by far the most common metamorphic volatiles, the *X* in most *T-X* diagrams is the mole fraction of CO_2 (or H_2O) in H_2O-CO_2 mixtures. Thus $X_{CO_2} = n_{CO_2}/(n_{CO_2} + n_{H_2O})$, where *n* is the number of moles or molecules of each species in the fluid mixture. *T-X*$_{fluid}$ diagrams, however, can be created for any volatile mixtures desired. In common *T-X*$_{fluid}$ diagrams, temperature is the ordinate (*y*-axis), and X_{CO_2} or X_{H_2O} is the abscissa (*x*-axis). Because pressure is also an important variable, a *T-X*$_{fluid}$ diagram must be created for a specified pressure.

Figure 4 is a T-X_{H_2O} diagram for Reaction (5) in which P_{lith} = 0.5 GPa, calculated with the same assumptions as Figure 2 ($P_{fluid} = P_{lith}$, and diluting H_2O ideally). In Figure 2, I have drawn a dashed isobaric line at 0.5 GPa and shown the intersection of this line with the series of equilibrium curves as a sequence of dots. These dots correspond to the dots in Figure 4 because $p_{H_2O} + p_{CO_2} = p_{lith}$ in a binary H_2O-CO_2 mixture (CO_2 dilutes H_2O), and ideal mixing assumes $p_{H_2O} = X_{H_2O} \cdot P_{fluid}$ (Dalton's law of partial pressures for ideal mixtures of gases).

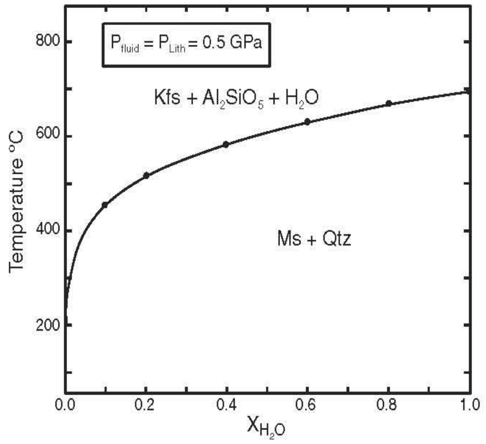

FIGURE 4 T-X_{H_2O} phase diagram for the reaction Ms + Qtz = Kfs + Sil + H_2O at 0.5 GPa, assuming ideal H_2O-CO_2 mixing, calculated using the program TWQ by Berman (1988, 1990, 1991). The dots correspond to those in Figure 2.

Once the equilibrium curve is plotted in Figure 4, it is easy to label the fields by remembering that the hydrous mineral assemblage is stable at low temperature, and the volatile phase is liberated as temperature increases. Note also that the maximum stability temperature of the hydrous assemblage is for pure H_2O (X_{H_2O} = 1.0), because this is the maximum p_{H_2O} possible at the pressure specified, and we can imagine optimal H_2O being forced into the hydrous muscovite, enhancing the mineral's stability. At very low p_{H_2O} there is little H_2O pressure, so muscovite breaks down. A hydrous phase is not stable in an absolutely H_2O-free environment, so the equilibrium curve never really reaches X_{H_2O} = 0, but becomes asymptotic to it at low temperature.

The shape of *all* dehydration curves on *T-X*$_{fluid}$ diagrams is similar to the curve in Figure 4. They have a maximum temperature at the pure H_2O end and a slope that is gentle at high X_{H_2O}, but increasingly steep toward low X_{H_2O}, becoming nearly vertical at very low X_{H_2O}. The temperature of the reaction can thus be practically any temperature below the maximum representing $p_{H_2O} = P_{lith}$. For most of the X_{H_2O} range in Figure 4, however, the reaction temperature varies by less than 200°C. Nonetheless, *one should take great care to constrain the fluid composition, if at all possible, before using a devolatilization reaction to indicate metamorphic grade.*

Decarbonation reactions may be treated in an identical fashion. For example, the reaction:

$$\underset{\text{Cal}}{CaCO_3} + \underset{\text{Qtz}}{SiO_2} = \underset{\text{Wo}}{CaSiO_3} + CO_2 \qquad (6)$$

can be shown on a T-X_{CO_2} diagram and has the same form as Reaction (5), only the maximum thermal stability of the assemblage containing the carbonate mineral occurs at X_{CO_2} = 1.0 (Figure 5). The temperature of a wollastonite-in isograd based on this reaction obviously depends upon p_{CO_2} in the same fashion as Reaction (5) depends upon p_{H_2O}.

In his theoretical and experimental study of the MgO-SiO_2-H_2O-CO_2 system, Greenwood (1967a) distinguished

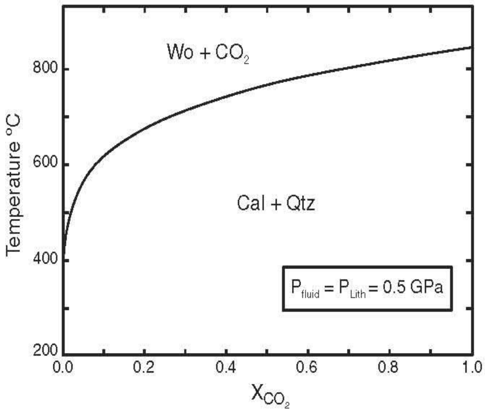

FIGURE 5 T-X_{CO_2} phase diagram for the reaction Cal + Qtz = Wo + CO_2 at 0.5 GPa, assuming ideal H_2O-CO_2 mixing, calculated using the program TWQ by Berman (1988, 1990, 1991).

five principal types of equilibria involving CO_2-H_2O fluids [other than those that conserve the volatile species, such as Reaction (4)]. Each type has its own characteristic shape on T-X_{fluid} diagrams. The five types are based on which volatile component is consumed or liberated *as temperature increases*:

1. Dehydration reactions, such as Reaction (5).
2. Decarbonation reactions, such as Reaction (6).
3. Combined dehydration–decarbonation reactions:

$$\underset{\text{Mgs}}{5\,MgCO_3} + \underset{\text{Tlc}}{Mg_3Si_4O_{10}(OH)_2} = \underset{\text{Fo}}{4\,Mg_2SiO_4} + 5\,CO_2 + H_2O \tag{7}$$

4. Prograde reactions that consume H_2O and liberate CO_2:

$$\underset{\text{Mgs}}{3\,MgCO_3} + \underset{\text{Qtz}}{4\,SiO_2} + H_2O = \underset{\text{Tlc}}{Mg_3Si_4O_{10}(OH)_2} + CO_2 \tag{8}$$

5. Prograde reactions that consume CO_2 and liberate H_2O:

$$\underset{\text{Zo}}{2\,Ca_2Al_3Si_3O_{12}(OH)} + CO_2 = \underset{\text{An}}{3\,CaAl_2Si_2O_8} + \underset{\text{Cal}}{CaCO_3} + H_2O \tag{9}$$

The typical shapes of these reaction types on T-X_{fluid} diagrams are illustrated in Figure 6. The shapes make some intuitive sense when considered in light of hydrous phases breaking down at very low X_{H_2O} and carbonate phases breaking down at very low X_{CO_2}. For example, in type 4 reactions, the mineral assemblage (A) in Figure 6 must include a carbonate mineral (because CO_2 is on the opposite side of the reaction). The carbonate-bearing assemblage breaks down along an isothermal traverse in Figure 6 toward the H_2O-rich end because there is little CO_2 to stabilize the carbonate. Assemblage (B), on the other hand, includes a hydrous mineral, which breaks down toward the CO_2-rich end. In type 5 reactions, (A) includes a hydrous phase, which breaks down toward low X_{H_2O}, and (B) includes a carbonate, which breaks down toward low X_{CO_2}. In reactions of type 3, assemblage (A) includes both a hydrous phase and a carbonate phase. The hydrous phase breaks down toward high X_{CO_2}, and the associated carbonate is consumed by the reaction even though it would otherwise be stable. Similarly, the carbonate breaks down at high X_{H_2O}, consuming the associated hydrous phase. There must be a thermal maximum to type 3 reactions in a T-X_{fluid} diagram. Any reaction that does not liberate or consume H_2O or CO_2 will not be affected by X_{CO_2} and will thus form a horizontal line on a T-X_{fluid} diagram.

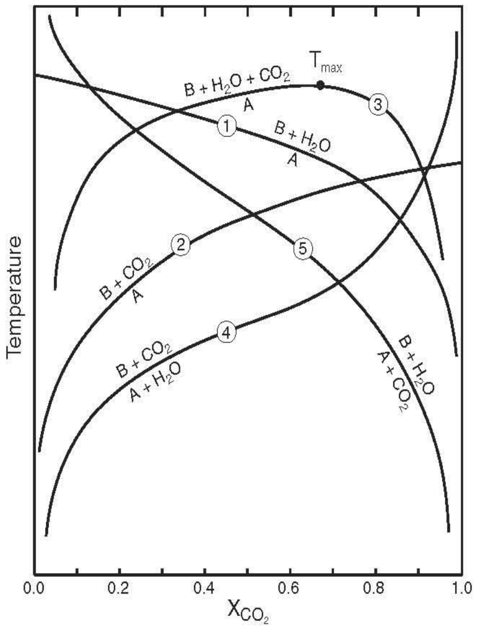

FIGURE 6 Schematic T-X_{CO_2} phase diagram, illustrating the general shapes of the five types of reactions involving CO_2 and H_2O fluids. *A* and *B* represent one or more solid phases, and reaction stoichiometry is ignored. After Greenwood (1967a). Copyright © reprinted by permission of John Wiley & Sons, Inc.

Greenwood (1967a) demonstrated theoretically that the location along the X-axis of the thermal maximum (T_{max}) of type 3 reactions is determined by the ratio of the stoichiometric coefficients of CO_2 and H_2O in the reaction (at least for ideal mixing behavior). If equal molar quantities of CO_2 and H_2O are liberated, T_{max} occurs at $X_{CO_2} = 0.5$. For Reaction (7), which liberates 5 moles of CO_2 for each mole of H_2O, T_{max} is located at $X_{CO_2} = 5/(5 + 1) = 0.83$ (assuming ideal CO_2-H_2O mixing). T_{max} for the reaction illustrated by the hypothetical curve (type 5) in Figure 6 is at $X_{CO_2} = 0.67$, indicating a reaction of the type $A = B + 2CO_2 + H_2O$.

Devolatilization reactions involve a potentially mobile fluid, and thus the pressure, temperature, and progress of these reactions depend on such physical rock properties as porosity and permeability. Recall the distinction between perfectly mobile versus less mobile fluid components. When a system is permeable, the fluids are free to migrate and are thus highly mobile. In such cases, fluids released from greater depths may pass through shallower rocks, which may be treated as **open systems** with respect to those fluids. If the external fluid reservoir is large with respect to the shallower system, and fluids pass through readily, the fluid composition may be controlled by the larger external reservoir and thus affect the mineral assemblage of the more shallow one. When permeability is low, on the other hand, fluids remain local and are more likely to equilibrate with the minerals present, so that the mineral assemblage of the shallow system controls the fluid composition and not vice versa. As an example of open-system behavior, imagine the nominal effect of your breathing on the composition of the air around you in a breezy open field. For a closed system, imagine the same effect if you were shut in a small, air-tight container.

For an example of how this concept might work during metamorphism, consider Figure 7, which illustrates two devolatilization reactions. The low-temperature reaction

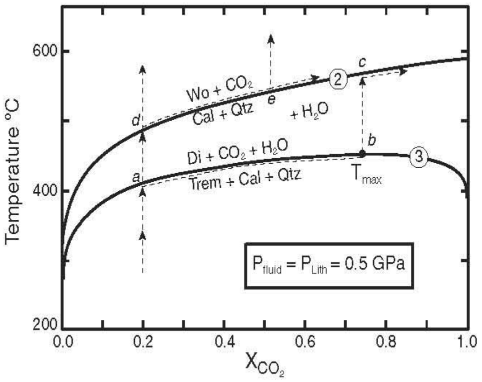

FIGURE 7 T-X_{CO_2} phase diagram in the CaO-MgO-SiO_2-H_2O-CO_2 system, for the reactions Cal + Qtz = Wo + CO_2 and and Tr + 3 Cal + 2 Qtz = 5 Di + 3 CO_2 + H_2O at 0.5 GPa, assuming ideal mixing of non-ideal gases, calculated using the program TWQ by Berman (1988, 1990, 1991).

is Reaction (5), a decarbonation reaction of type 2 above, and the other is:

$$\underset{\text{Tr}}{Ca_2Mg_5Si_8O_{22}(OH)_2} + 3\,\underset{\text{Cal}}{CaCO_3} + 2\,\underset{\text{Qtz}}{SiO_2} = 5\,\underset{\text{Di}}{CaMgSi_2O_6} + 3\,CO_2 + H_2O \qquad (10)$$

a type 3 reaction that liberates both H_2O and CO_2. Because the molar ratio of CO_2:H_2O liberated in Reaction (10) is 3:1, T_{max} occurs at $X_{CO_2} = 3/(3 + 1) = 0.75$ in Figure 7. Other reactions occur in the CaO-MgO-SiO_2-H_2O-CO_2 system, and may affect the reactions considered here and play an important role in meta-carbonate petrogenesis. They are ignored for the sake of simplicity in the present discussion so that we can focus on fluid behavior associated with some representative reactions rather than what mineral assemblage actually develops.

Suppose we begin with a marble that contains calcite + quartz + tremolite at low temperature (already above the tremolite isograd that has been left out of the diagram) and that the initial intergranular fluid phase is composed of 20 mol % CO_2 and 80 mol % H_2O. If we heat this mixture, the fluid follows the vertical arrow at $X_{CO_2} = 0.2$. At about 410°C, the system reaches the equilibrium curve for Reaction (10) (point a), and Tr + Cal + Qtz react to form diopside, liberating 3 moles of CO_2 and 1 mole of H_2O for each mole of tremolite consumed. First, let's assume that the rock is porous and permeable (*open-system* behavior), so these volatile species are free to escape and leave the system without altering the composition of the intergranular fluid phase that passes through the rock, which would then remain at $X_{CO_2} = 0.2$ if it is controlled at that composition by some large external reservoir. If this is the case, Reaction (10) will behave as an invariant (discontinuous) reaction. According to the phase rule, $F = C - \phi + 2 = 5 - 5 + 2 = 2$, but, because P and X_{CO_2} are externally fixed, F is reduced by 2, to 0. Alternatively, we could consider CO_2 and H_2O as perfectly mobile, so $C = 3$ and $\phi = 4$ (you can't count the fluid phase if you don't count CO_2 and H_2O as components). Thus $F = 3 - 4 + 1$ (isobaric) $= 0$. Because the reaction is invariant, the system will remain at 410°C (and $X_{CO_2} = 0.2$) until the reaction runs to completion (defined as the point at which *one of* the reactant phases is consumed; remember that a reaction can proceed only as long as *all of* the reactants are present). Any heat added while $F = 0$ is consumed by the endothermic reaction at a constant temperature.

Once a reactant is consumed, the reaction is considered complete, and temperature may rise again along the fixed X_{CO_2} fluid path. If tremolite is the limiting phase and is consumed first, the system may be heated to point d, where the remaining calcite and quartz will react to produce wollastonite via Reaction (5) and liberate only CO_2. Again, if the fluid is perfectly mobile and controlled by an external reservoir at $X_{CO_2} = 0.2$, then this too will act as a discontinuous invariant reaction (in the CaO-SiO_2-CO_2 system) and remain at 487°C until either calcite or quartz is consumed before the temperature can rise again with Wo + Qtz or Wo + Cal present.

Alternatively, if the initial temperature were around 350°C and $X_{CO_2} = 0.2$, but nearly pure H_2O fluids were released into the shallow system from a crystallizing granite below, X_{CO_2} would then decrease to approximately zero, causing both "prograde" reactions to occur, producing first diopside and then wollastonite *under isothermal conditions*. Such a process may be responsible for the occurrence of very wollastonite-rich rocks associated with numerous marbles. Tracy et al. (1983) described a situation in Connecticut where quartz veins inject marble lenses and created calc-silicate assemblages at the boundaries. They interpreted the veins as representing externally controlled SiO_2-H_2O-rich fluid conduits, and the addition of H_2O caused the marble to decarbonate locally, producing the calc-silicate assemblages at the margins.

Next consider a situation in which the permeability is limited. If the original Cal + Tr + Q is heated to point a, Reaction (10) produces $CO_2:H_2O$ in the ratio of 3:1, which is richer in CO_2 than the initial fluid ($X_{CO_2} = 0.2$). If the permeability is low, the fluid produced by the reaction mixes with the original fluid, shifting X_{CO_2} to higher values. Because the reaction tremolite + calcite + quartz → diopside has already begun in order to accomplish this fluid shift, all four mineral phases are present, so the fluid cannot simply shift isothermally to the right of the univariant equilibrium curve on the T-X_{fluid} diagram because this would require losing Di again. Rather, the path must *follow the equilibrium reaction curve* along the dashed line (offset slightly for clarity). This is a classic **buffer** process, in which the solid mineral assemblage controls, or buffers, the fluid composition. Because X_{fluid} is no longer fixed, $F = 1$ (in an *isobaric* system). As long as all four solids and fluid coexist (at a particular pressure), *the fluid composition is determined by the temperature*, along the equilibrium curve in Figure 7. If we continue to heat the system, the composition of the fluid will be buffered toward higher X_{CO_2} as temperature rises and the reaction proceeds, consuming Tr, Cal, and Q and producing Di and CO_2-enriched fluid over that interval. The reaction is thus a univariant one and occurs over a temperature interval across which the proportions of the reactants and products vary.

At what point will a buffering reaction cease? It depends upon the quantities of the reactants and fluid and the permeability of the rock. The porosity is probably very small in most regionally metamorphosed rocks and restricted to an intergranular film (less than 1 to 2% of the rock volume). In such a case, growth of only a few volume % of diopside would release over 10% fluid, which would greatly modify (and perhaps flush out) the small amount of fluid initially present. The prograde reaction will thus modify the fluid toward $X_{CO_2} = 0.75$ as the temperature rises toward T_{max} at 455°C (point b on Figure 7). Suppose such a system evolves to point b. At this point, the fluid produced by the reaction is equal to the existing pore fluid, and neither the temperature nor the fluid composition can change as long as all four minerals are present. Thus the reaction will run to completion at 455°C, until one reactant is consumed. Greenwood (1975) argued that this should be a common situation and that even though a reaction path such as $a \rightarrow b$ in Figure 7 spans approximately 45°C as it progresses along the Di-producing reaction, only a minor amount of Di is created until X_{CO_2} of the fluid is stabilized at 0.75. If Greenwood is correct, the reaction will produce and maintain a reservoir of fluid with $X_{CO_2} = 0.75$ at point b during most of the reaction process. This, in turn, is capable of "externally buffering" the fluid for other rocks (generally situated above this system because fluids tend to rise). A similar external buffer may have been responsible for maintaining $X_{CO_2} = 0.2$ in the open system described above.

Once a reactant is consumed, the temperature of the system may rise from the equilibrium curve for Reaction (10). Again, if tremolite is consumed first, calcite + quartz will react to wollastonite at point c, where pure CO_2 is produced at 570°C. In the case of low permeability, the Cal + Qtz + Wo assemblage will then buffer the fluid with rising temperature toward $X_{CO_2} = 1.0$. Again, if Greenwood (1975) is correct, the generation of very little Wo may be required to raise X_{CO_2} of the fluid to nearly 1.0, and most of the Wo will be created when the fluid composition becomes stabilized at that composition at around 590°C.

If one of the reactants is present in very small quantities, or if the rock is semi-permeable, either reaction may run to completion before the composition of the pore fluid becomes stabilized at the value of the fluid produced by the reaction. Is such situations, the reaction (and its buffering ability) will cease at some point along the reaction-buffering path before reaching T_{max}. For example, Reaction (10) may cease when tremolite (or another reactant) is consumed before X_{CO_2} of the fluid reaches 0.75 in Figure 7. The T-X_{fluid} path of the process may thus leave a reaction curve at any point between the point it first encounters the equilibrium curve and the ultimate stabilized fluid composition.

It is generally impossible to predict at what T-X_{fluid} point a devolatilization reaction will run to completion. The open-system and buffer-to-T_{max} scenarios represent the two extreme situations. Even in low-porosity, well-buffered situations, such as the path $a \rightarrow b$ in Figure 7, as the composition of the intergranular fluid approaches point b during the progress of Reaction (10), more reaction progress is required to modify it because the fluid being produced is approaching that already existing in the pore spaces. Greenwood (1975) may be correct in that only a small degree of reaction progress is required to buffer the fluid composition quickly to the *vicinity of* T_{max}. The reaction, however, may still run to completion before it finally gets there.

So the temperature interval over which a buffered reaction takes place is wider than for unbuffered open systems. Rather than having the reactants and products coexist only at a single temperature (open system, discontinuous) they can coexist over a temperature range, in many cases in excess of 100°C. As with regard to periclase, brucite, and H_2O, the fluid phase is not perfectly mobile in buffered situations, and thus H_2O and CO_2 must be considered as components, and the fluid considered as a phase, thereby explaining why so many phases (reactants plus products) coexist over a temperature interval (and perhaps across a modest spatial zone). Rather than being discontinuous, the reactions become continuous, as the composition of at least one phase (in this case, the fluid) changes over the temperature interval in which the reaction proceeds. Such metamorphic continuous reactions are analogous to continuous melting reactions. We shall develop this concept further in the next section, when we generalize to include solid-solutions as well.

5 CONTINUOUS REACTIONS

Imagine an idealized field area of steeply dipping metamorphosed, mostly pelitic sediments that strike directly up metamorphic grade (Figure 8). The bulk composition of each unit is homogeneous but differs somewhat from the other units in the area. One can thus compare how each composition behaves as the grade of metamorphism increases by walking within each unit along strike toward higher grade. The garnet isograd (based on the first appearance of garnet) is shown in Figure 8 as a dashed line. Note that the isograd is not located at the same grade in each unit. This may occur for one of two reasons (assuming that the rocks represent equilibrium mineral assemblages):

1. The rocks may be of such contrasting compositions that garnet is produced by different reactions. For example, in some rocks, garnet may be created by the (unbalanced) reaction:

$$\text{Chl} + \text{Ms} + \text{Qtz} \rightarrow \text{Grt} + \text{Bt} + H_2O \qquad (11)$$

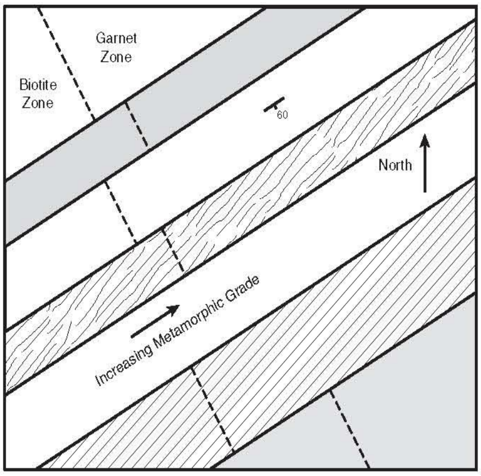

FIGURE 8 Geologic map of a hypothetical field area in which metamorphosed pelitic sediments strike directly up metamorphic grade. The isograd based on the first appearance of garnet is shown as a dashed line. The offsets of this isograd at unit contacts are discussed in the text.

In more Fe-rich and K-poor pelites, garnet might be generated by an (unbalanced) reaction involving chloritoid:

$$\text{Chl} + \text{Cld} + \text{Qtz} \rightarrow \text{Grt} + H_2O \qquad (12)$$

Offsets in a particular isograd, when based on different reactions, may be relatively large. In the blank unit in the center of the map, garnet isn't created at all. This could be a Mg-rich sandy pelite or even a quartzite or marble.

2. The reaction on which the isograd is based is the same in each unit, but it is a **continuous reaction**, and its location is sensitive to the composition of the solutions (either solid or fluid) involved. The offsets this creates in an isograd are usually more subtle than for reason #1, but in some cases they can be substantial.

Isograd offsets due to the first reason are relatively obvious. For now, let's concentrate on the second reason.

To understand the effect of solutions on the temperature of an isograd, let's go back to a familiar system: the Fo-Fa solid solution that comprises olivine in Figure 23. Notice that the temperature at which melt first occurs depends on the Mg/Fe ratio of the bulk composition that we plan to melt. If we begin with a rock that has 30 wt. % Fo, for example, melt of a composition having about 8 wt. % Fo is first generated at ~1320°C. If we begin with a rock that has 70 wt. % Fo, on the other hand, melt with a composition of about 35 wt. % Fo will first be generated at ~1585°C. The temperature at which melt is first generated (consider it a "melt-in" isograd) between these two examples varies by about 265°C!

While we are referring to Figure 23, it may be a good time to recall the difference between discontinuous and continuous reactions. A *discontinuous* reaction occurs at a constant temperature when there are no degrees of freedom ($F = 0$) according to the phase rule. As an example, consider pure forsterite at a constant pressure in Figure 23. In the pure system, the number of components, C, is 1. When forsterite begins to melt at 1890°C, $\phi = 2$, so that $F = C - \phi + 1(isobaric) = 1 - 2 + 1 = 0$. Thus the temperature remains constant until all of the forsterite is consumed by the melting reaction. This is discontinuous because a pronounced change occurs in the system at a single temperature (solid below the temperature, liquid above it).

In the two-component system, if we similarly heat Fo_{30}, melting begins at 1320°C but is not completed until 1535°C, at which time the liquid composition becomes equal to the bulk composition. In this case, the melting reaction is a *continuous* reaction because $C = 2$ and $F = 2 - 2 + 1 = 1$. Because there is a degree of freedom, temperature is free to vary, and the composition of the liquid and solid varies along the liquidus and solidus, respectively, as melting progresses.

So, discontinuous reactions occur at a constant temperature (or metamorphic grade). Discontinuous reactions are actually *univariant* ($F = 1$) on *P-T* phase diagrams. Because pressure and temperature are not independent during metamorphism, however, but constrained to follow a geothermal gradient or *P-T-t* path, the *P-T* path thus crosses the reaction at a single *P-T* point. In other words, because T depends upon P (as determined by the local geothermal gradient), a degree of freedom is lost. Suppose Reaction (11) were a discontinuous reaction (let's say it occurred for pure Mg end-members) and is responsible for the formation of garnet in the map area of Figure 8. We would then expect the reaction to run to completion (when *one* of the reactants was consumed) at a single metamorphic grade. Continuous reactions occur when $F \geq 1$, and the reactants and products coexist over a temperature (or grade) interval. If Reaction (11) were a *continuous* reaction, then we would expect to find chlorite, muscovite, quartz, biotite, and garnet all together in the same rock over an interval of metamorphic grade above the garnet isograd. The composition of one or more solution phases (usually all of them) will then vary across the interval, and the proportions of the minerals will change correspondingly until *one of* the reactants disappears with increasing grade.

A continuous metamorphic reaction is illustrated in Figure 9, a schematic *isobaric* $T\text{-}X_{Mg}$ representation of Reaction (11), simplified to eliminate K_2O and approximate a two-component system analogous to the Fo-Fa melting reaction in Figure 23. The reaction is discontinuous in the pure Fe and pure Mg systems, but continuous in the mixed Fe-Mg system (C increases by one, so F does also). Just as in Figure 23, the absolute temperature of the first appearance of the new phase (garnet), as well as the width of the temperature interval within which the reactants and products coexist, varies with the Fe/Mg ratio of the bulk rock composition. For the pure-Fe and pure-Mg systems, the reaction occurs at a single temperature (T_{Fe} or T_{Mg}), and the reaction curves on a *P-T* diagram (dashed in Figure 9b) are sharp (discontinuous), univariant reactions crossed at a single grade. For a mixed Fe/Mg system, however, the

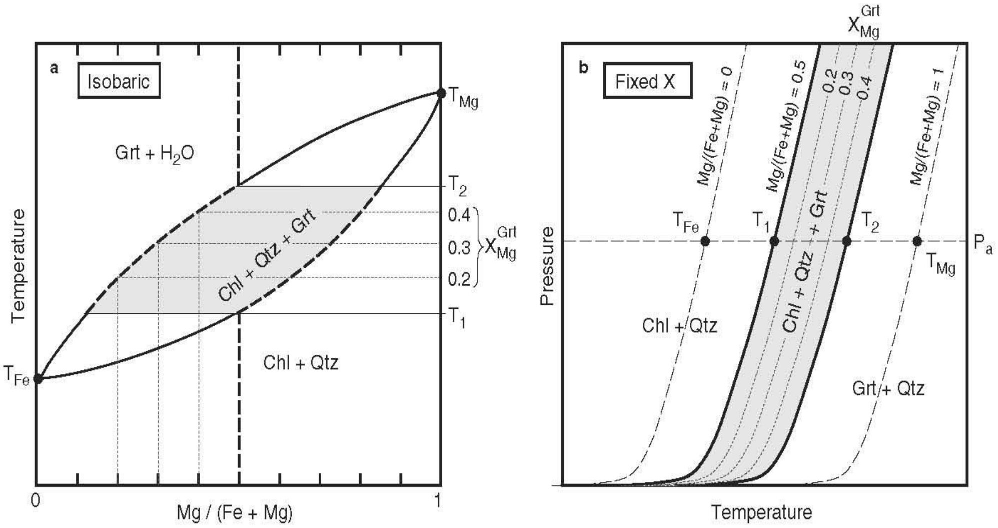

FIGURE 9 **(a)** Schematic isobaric T-X_{Mg} “pseudosection” representing the simplified metamorphic reaction Chl + Qtz → Grt + H_2O. **(b)** Schematic P-T “pseudosection” for a specific bulk composition [in this case for Mg/(Mg + Fe) = 0.5 and quartz-excess], showing the stability fields of Chl + Qtz, Chl + Qtz, and Grt + Qtz. Note the continuous nature of the reaction when all solid phases are present (shaded area). Note also that one can contour the shaded divariant field in (b) for specific compositions of either garnet (as has been done) or chlorite. The boundaries and contours would change for a different X_{bulk} (i.e., different X_{Mg}), and even the field assemblages might change: for example, the higher-temperature garnet + quartz field would be garnet + chlorite if the SiO_2 content were so low that quartz were consumed before chlorite by the reaction.

reaction becomes continuous. Suppose, for example, a rock with Mg/(Fe + Mg) = 0.5 is heated (vertical heavy dashed line at the bottom of Figure 9a). The garnet-in isograd for such a rock occurs at T_1. Chlorite (or quartz in less common SiO_2-poor pelites) is not consumed until T_2 is reached. Between T_1 and T_2, the Chl + Qtz (+ Ms) → Grt + H_2O (+ Bt) reaction is continuous, all five minerals are present, and chlorite is gradually consumed as more garnet is produced while the composition of each becomes progressively more Mg-rich (although X_{Mg} at any given temperature is not the same in garnet as it is in biotite or chlorite). On a P-T phase diagram (Figure 9b), the reaction for $X_{Mg} = 0.5$ is shown as the shaded band. If isothermally heated, T_1 is the garnet-in isograd, and chlorite is consumed at T_2. A more likely situation would involve a P-T-t path with positive slope rather than being isothermal, but T_1 and T_2 would nonetheless be fixed by the intersection of the path and the reaction boundaries. Figures 9a and b constitute rudimentary T-X and P-T **pseudosections**: grids designed to show reactions *for specific rock compositions*. A hallmark of pseudosections is the depiction of fields of stability of particular mineral assemblages, rather than showing the univariant, typically pure-Mg or pure-Fe, end-member reactions so common on P-T grids. The isograd offsets mapped in Figure 8 may thus reflect differences in bulk X_{Mg} from one unit to another (imagine any other bulk composition in Figure 9a), and the continuous reaction proceeds across a variable width within the garnet zone immediately above each isograd segment.

When petrologists use the term *continuous reaction*, they are referring to reactions such as the one illustrated in Figure 9, involving *solid* solutions. Devolatilization reactions may be continuous as well, in a sense, because the *fluid* composition may change over a buffered reaction temperature interval. Only when a devolatilization reaction is *also* affected by continuous *solid*-solution behavior would the reaction be considered “continuous” in common usage (as is the case for the reaction in Figure 9).

6 ION EXCHANGE REACTIONS

Ion exchange reactions involve the reciprocal exchange of components between two or more minerals. Although the exchange can involve anions or anionic complexes, such as Cl-F-OH exchange among amphiboles and micas, petrologists have concentrated more on exchange reactions involving cations. Typical examples include:

Fe-Mg exchange between Opx and Cpx:

$$\text{En} + \text{Hd} = \text{Fs} + \text{Di}$$

Fe-Mg exchange between garnet and biotite:

$$\text{Annite} + \text{Pyrope} = \text{Phlogopite} + \text{Almandine}$$

Note that ion-exchange reactions are conveniently expressed in terms of the opposing pure end-member components ($A_{Fe} + B_{Mg} = A_{Mg} + B_{Fe}$), and an equilibrium constant is then fitted to actual compositions.

Although continuous reactions may also involve shifting Fe/Mg ratios in reacting phases, the modal proportions of the phases also change as a continuous reaction progresses. Ion exchange reactions differ in that *the modal* *amounts of the phases involved remain constant*; only their composition changes as a result of the exchange. We have become increasingly aware of these adjustments in the past 30 years because of the relative ease of determining mineral compositions using the electron microprobe.

The partitioning of cations between two minerals in equilibrium is significantly temperature dependent. Many of the exchanges have been experimentally calibrated, and the compositions of coexisting phases have been used to estimate the temperature or pressure of metamorphic equilibration, leading to the technique known as *geothermobarometry*. The fixed distribution of Fe and Mg, for example, on an *AFM* diagram representing a given metamorphic grade requires that the *tie-lines connecting coexisting phases cannot cross*. Exchange reactions occur as grade changes and cause the tie-lines to rotate as Fe and Mg ratios vary. The tie-lines representing one temperature may thus cross those representing another temperature. Crossing tie-lines, when observed between coexisting solid solutions in a single rock, are good indicators of non-equilibrium, such as partial readjustments to changing grade.

Exchange reactions can occur readily, even during retrograde metamorphism, a process that can significantly upset geothermobarometry. A common example is biotite in high-temperature rocks that cool slowly. When a rock is in equilibrium, the composition of any particular mineral should be the same throughout the rock. If a mineral is zoned, the rim, at least, should be in equilibrium with the rims of the other minerals. Biotite rim compositions in numerous high-grade gneisses vary somewhat, depending on the mafic mineral with which the biotite crystal is in contact. This suggests that some limited exchange occurred during cooling. The temperature determined by a geothermometer involving biotite may thus record a **blocking** or **closure temperature** (the temperature below which kinetic factors impede the retrograde exchange reaction), rather than the metamorphic peak temperature. For cases in which the biotite compositions vary, it may be better to analyze a biotite surrounded by felsic minerals where retrograde Fe-Mg exchange with an adjacent mafic neighbor cannot readily occur.

7 OXIDATION/REDUCTION REACTIONS

Oxidation/reduction, or **redox**, reactions involve changes in the oxidation state of ions or ionic complexes that naturally occur in more than one state. Fe^{2+}-Fe^{3+} is probably the most common multi-valent ion of geological interest, but other examples include Cu^{+}-Cu^{2+}, Mn^{2+}-Mn^{3+}, O^{0}-O^{2-}, S^{0}-S^{2-}, C^{0}-C^{4+}, etc. A simple redox reaction that relates hematite and magnetite is:

$$6\,Fe_2O_3 = 4\,Fe_3O_4 + O_2 \qquad (13)$$

In this reaction, two-thirds of the Fe^{3+} ions in hematite are reduced to Fe^{2+} ions in magnetite, and half as many O^{2-} ions are oxidized to O^{0} to compensate and maintain electrical neutrality. Notice that, in the three-component system FeO-O_2-H_2O (H_2O is added so that oxygen pressure can vary), the occurrence of three phases at equilibrium requires that $F = 3 - 3 + 2 = 2$. Because magnetite and hematite are pure phases, only P, T, and p_{O_2} are variable. At any particular pressure, the solid assemblage hematite + magnetite requires that $F = 1$, and the assemblage behaves as an **oxygen buffer**: imposed changes in oxygen concentration are compensated by shifting the relative proportions of hematite and magnetite at equilibrium. The equilibrium reaction curve can be plotted on an isobaric T-p_{O_2} diagram (Figure 10). This diagram uses oxygen *fugacity* (f_{O_2}) instead of partial pressure. Fugacity is the thermodynamically effective pressure and can be substituted for partial pressure if the difference between real and ideal behavior can be determined in the lab. Two other oxygen-buffering reactions are included in Figure 10. These are:

$$2\,Fe_3O_4 + 3\,SiO_2 = 3\,Fe_2SiO_4 + O_2 \qquad (14)$$

$$\text{magnetite} + \text{quartz} = \text{fayalite ("FMQ")}$$

$$Fe_2SiO_4 = 2\,Fe^{0} + SiO_2 + O_2 \qquad (15)$$

$$\text{fayalite} = \text{iron} + \text{quartz ("QIF")}$$

Although these buffers are effective at controlling oxygen fugacity in experimental runs, natural rocks are more complex and in many cases control f_{O_2} by equilibria involving several silicate and/or oxide phases. Only in ironstones does the hematite–magnetite (HM) buffer operate approximately as advertised. Nevertheless, the buffers in Figure 10 bracket natural f_{O_2} values in metamorphic and igneous rocks because Fe in silicates is seldom as oxidized as in hematite, and it is rarely found in the native iron state. Notice that this limits f_{O_2} values in metamorphic rocks (shaded area in Figure 10) to the range of 10^{-10} to 10^{-50} MPa. This may be as little as a few molecules of free O_2 per cubic cm of rock! When present in such minute amounts, oxygen may not be able to diffuse easily through the rock, and values of f_{O_2} may thus vary on a local

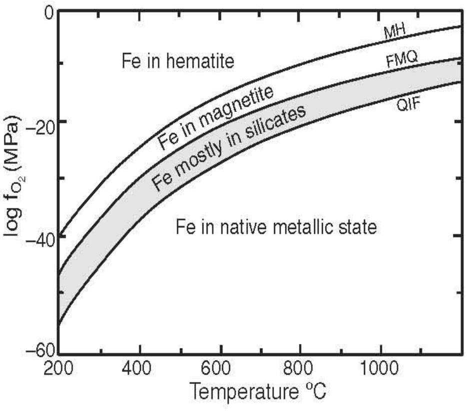

FIGURE 10 Isobaric T-f_{O_2} diagram showing the location of Reactions (13) to (15) used to buffer oxygen in experimental systems. Note the range of f_{O_2} in which iron occurs principally in silicate minerals (i.e., most natural rocks). After Frost (1991). Copyright © the Mineralogical Society of America.

basis. This would explain, for example, why banded iron formations have sub-centimeter-scale layers of hematite and magnetite between which f_{O_2} varies considerably.

Redox reactions are common in a number of metamorphic, igneous, hydrothermal, and near-surface aqueous systems. The presence of carbonaceous material in many dark shales is a powerful reducing agent, resulting in some reduced meta-pelite mineral compositions. For a summary of redox reactions, see a geochemistry text, such as Faure (1998), and for a more specific review of redox in metamorphism, see Eugster (1959).

8 REACTIONS INVOLVING DISSOLVED SPECIES

Fluids are capable of dissolving a variety of chemical components as they equilibrate with the minerals in a rock. These components are garnered by reactions between the fluids and minerals, and the dissolved species are generally maintained in equilibrium with the solids, unless the flow rate is too fast and/or the fluids are buffered by some larger external reservoir. The approach to equilibrium between a fluid and the minerals of a rock is generally referred to as **fluid–rock interaction**. This interaction is fundamental to the process of metasomatism and is also important during regional metamorphism, weathering, ore deposition, hydrothermal alteration, ocean-floor metamorphism, etc.

A well-used example of this type of reaction is the **hydrolysis** weathering reaction of K-feldspar given in practically every introductory geology text:

$$\underset{\text{Kfs}}{2\,\mathrm{KAlSi_3O_8}} + \underbrace{2\,\mathrm{H^+} + \mathrm{H_2O}}_{\text{aqueous species}} \tag{16}$$

$$= \underset{\text{kaolinite}}{\mathrm{Al_2Si_2O_5(OH)_4}} + \underbrace{\mathrm{SiO_2} + 2\mathrm{K^+}}_{\text{aqueous species}}$$

By this reaction, orthoclase reacts with somewhat acidic H_2O to form a common clay mineral plus dissolved SiO_2 and K^+ ions. As another example, the albitization of plagioclase during ocean-floor metamorphism involves the substitution of Na^+ dissolved in seawater for Ca^{2+} in the anorthite component of the plagioclase (plus other mineral products).

Many metamorphic reactions involve such aqueous constituents. The reactions may be understood in terms of the phase rule and the appropriate intensive variables: typically T, P, and the concentrations of the aqueous species. Isobaric T-concentration diagrams, isobaric–isothermal concentration–concentration diagrams (e.g., C_{H^+} versus C_{K^+} for Equation 16), or plots of T versus concentration ratios (e.g., T versus C_{K^+}/C_{H^+}) can be used in the same way as Figures 4 through 10. Activities (thermodynamically effective concentrations) are typically substituted for concentrations, resulting in T-activity or activity–activity diagrams. As we shall see in Section 11, even mineral reactions that do not appear to involve dissolved species in the overall reaction may have them as intermediate states. The "net transfer" in solid–solid net transfer reactions implies migration of such dissolved material. We shall postpone further discussion of reactions that involve dissolved species.

9 REACTIONS AND CHEMOGRAPHICS: A GEOMETRIC APPROACH

Chemographic diagrams can be excellent geometric aids that help conceptualize the relationship between rock chemical composition and stable equilibrium mineral assemblages. An appropriate chemographic compatibility diagram should be limited to a small range of P-T conditions, such as a metamorphic zone. The reason for this restriction is that zones are separated by isograd reactions, and reactions change the geometry of compatibility diagrams. Diagrams representing any two zones will thus appear different, having either different phases, different tie-lines connecting coexisting phases, or both. A change in tie-lines between adjacent metamorphic zones thus means that different mineral groupings result from the reaction that separates them. We typically refer to the overall geometry of phase compositions and tie-lines on a compatibility diagram with the general term **topology**.

To understand how reactions can be dealt with in terms of chemographic geometries, it is probably easiest to begin with a simple binary system. You may remember that three collinear phases on a chemographic phase diagram imply a possible reaction because the central phase can be generated by combining the phases at the ends of the line.

For example, consider the binary chemographic diagram in the MgO-SiO_2 system illustrated in Figure 11, which makes a good binary compatibility diagram. Specify a rock bulk composition by picking any point along the line, and the mineral assemblage that develops equals the two phases that bracket the point. SiO_2-rich rocks will thus develop En + Qtz, less SiO_2-rich rocks will develop Fo + En, and MgO-rich rocks will develop Per + Fo. We can combine any two phases on the diagram to create a phase between them, such as Per + En = Fo, or Fo + Qtz = En. The geometry indicates that these reactions are possible but does not indicate whether a reaction must occur in nature, nor the conditions under which it might occur (something requiring experimental or thermodynamic data). If we write down the formulas, we find that we can balance any reaction indicated geometrically. For example:

$$\underset{\text{Fo}}{\mathrm{Mg_2SiO_4}} + \underset{\text{Qtz}}{\mathrm{SiO_2}} = \underset{\text{En}}{2\,\mathrm{MgSiO_3}} \tag{17}$$

We could get the ratio of Fo:Q for the reaction directly from the chemographic diagram by using the lever principle, if necessary, but it's usually easier to balance the

FIGURE 11 An example of a possible chemographic diagram in the binary MgO-SiO_2 system, showing the positions of periclase, forsterite, enstatite, and quartz.

reaction mathematically. The simple geometric rule that two minerals can be combined to create a mineral that plots directly between them tells you whether a reaction *can be* balanced; the actual balancing is then a simple matter of bookkeeping.

So how would a compatibility diagram change from one zone to another via such a reaction? Suppose Reaction (17) is an "enstatite isograd" for some hypothetical field area. Below the isograd, the linear chemographic diagram might look like Figure 11, but it will have only periclase, forsterite, and quartz, whereas above the isograd Figure 11 would apply because enstatite is generated and appears on the line between Fo and Qtz. This example is purely hypothetical, of course, because forsterite and quartz never coexist at equilibrium in nature, contrary to the implication of the Fo-Qtz tie-line in the chemographics below our hypothetical "isograd." Alternatively, a reaction may signify the *disappearance* of a phase with increasing metamorphic grade (a "mineral-out" isograd), in which case the phase would appear in the lower-grade diagram and not in the one representing the higher grade.

A similar situation for three components is illustrated in Figure 12. From the geometry shown, we could infer that $A + B + C$ could be combined in some proportions to produce composition X because X is coplanar with A, B and C and lies within the A-B-C chemographic triangle. The triangle need not be equilateral and could be any sub-triangle within a larger three-component system. *As long as a phase lies within a triangle, the apices of which are three other phases, the apical phases could be combined to create the phase within.* Again, balancing the reaction is a matter of bookkeeping. The formula of X in Figure 12 is A_2BC, so the reaction would be $2A + B + C = X$.

The geometric implication of a point within a triangle for a possible reaction is true whether the triangle is a true ternary diagram or a **projection**. If the chemographic triangle is part of a projection, balancing it will require other phases and/or components (ones involved in the projection). For example, suppose the A-B-C triangle is a projection in some four-component system. If we "un-project" it and view it in three dimensions, it may appear as in Figure 13. Note that point X can be construed as either a combination of phases A, B, and C or as a linear combination of phases D and E. We can thus geometrically infer the (unbalanced) reaction: $A + B + C = D + E$. Such a reaction is possible because some combination of phases on both sides of the reaction can be equivalent to X. This is true for any line that pierces a triangle in chemographic space because the point of intersection can be resolved into either the corners of the coplanar triangle or the ends of the line.

A **"tie-line flip"** is perhaps the most common situation in which a reaction causes a change in topology for a chemographic diagram. Consider Figure 14, in which a hypothetical three-component system has six phases, A, B, C, D, X, and Y. Suppose Figure 14a represents a lower-grade metamorphic zone and Figure 14c represents an immediately higher grade zone. The possible mineral assemblages in part (a) are:

$X + A + D \quad A + D + B \quad A + B + C \quad B + D + Y$

But the assemblages in part (c) are:

$X + A + D \quad A + D + C \quad C + D + B \quad B + D + Y$

Notice that *the minerals in both diagrams are the same, but the groupings (tie-lines) differ*. Figure 14b shows the transitional situation at the isograd itself. Remember that coexisting phases are connected by tie-lines. The **crossed tie-lines** indicate the isograd reaction geometrically. Because the point of intersection of the two alternative tie-lines is an intermediate point on either line, it could be composed of either $A + B$ or $C + D$. This implies that the contrasting

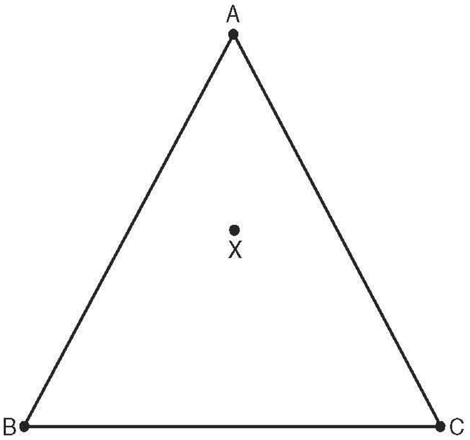

FIGURE 12 A hypothetical three-component system, *A*-*B*-*C*, having a compound *X* within the triangle. *X* can be generated by a reaction involving $A + B + C$.

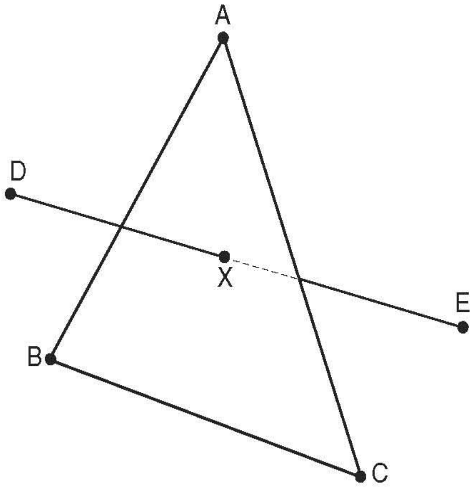

FIGURE 13 Three-dimensional perspective view of the *A*-*B*-*C* triangle in Figure 14, contained in a hypothetical four-component system. *X* can be generated by a combination of $A + B + C$ or of $D + E$, implying a possible reaction: $A + B + C = D + E$.

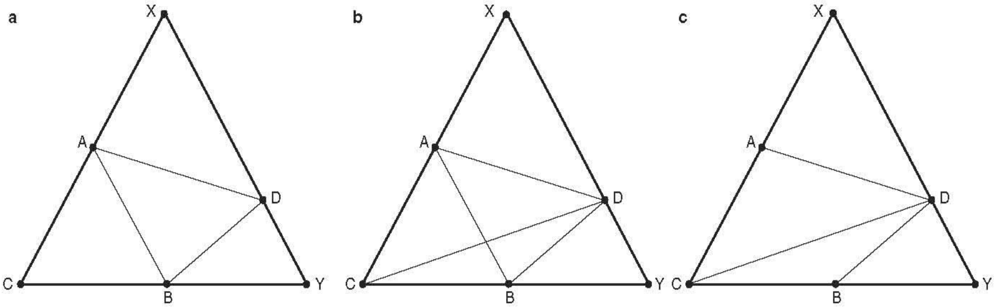

FIGURE 14 The sequence of chemographic diagrams for a hypothetical three-component system illustrating a "tie-line flip" resulting from a reaction $A + B = C + D$. **(a)** The topology for the lower grade. **(b)** The topology for the transition. **(c)** The topology for the higher grade.

pairs, if combined in the appropriate proportions, are compositionally equivalent, suggesting the (unbalanced) reaction:

$$A + B = C + D$$

The chemographic diagrams for the two zones (Figures 14a and c) are thus related by a "flip" of the *A-B* tie-line to become the *C-D* tie-line. When combined, the tie-lines cross, and this can be used to derive the reaction that relates the two zones. Once again, this is rigorously true only if the four phases at the ends of the tie-lines are indeed coplanar and not a projection. If they are projected, the reaction would be:

$$A + B + \ldots = C + D + \ldots$$

where the ellipses indicate that other phases, composed of the projected components, may be needed to produce a final mathematically balanced reaction. Again, the geometry of crossing tie-lines shows that a balanced reaction is possible, but it can't do the balancing for you.

More complex geometric reaction constructions are possible, including intersecting planes, etc., but the added complexity of visualizing in three or more dimensions soon compromises the advantages of the approach. The simple geometries discussed above are the most useful. For more complex reactions, an approach based on linear algebra is preferable for balancing. The program CSpace and the brief tutorial available via www.prenhall.com/winter may be used to balance any reaction that can be balanced.

10 PHASE DIAGRAMS FOR MULTICOMPONENT SYSTEMS THAT INVOLVE SEVERAL REACTIONS

Metamorphic reactions do not occur singly, in isolation from other reactions. For example, if we were to treat only the andalusite = kyanite reaction, we might assume that the reaction extrapolated as a straight line across the whole width of the diagram. Only when we consider all of the Al_2SiO_5 minerals (and pyrophyllite, when H_2O and silica are present in sufficient quantities) do we discover more accurately the stability of andalusite and kyanite in the Al_2SiO_5-SiO_2-H_2O system. As systems become more complex, containing four or more components, the phase diagrams become more complex as well. Pressure–temperature phase diagrams that show a host of reactions in a system are called *petrogenetic grids* (Section 11).

Before we look into examples of petrogenetic grids, let's first address a few simple rules that govern the way reactions behave when they intersect on phase diagrams. "Topology" may also be used to describe such geometric patterns of reaction curves. The rules follow the strictly geometric treatment of **Schreinemakers** (see Zen, 1966, for a complete description of the method, or Powell, 1991, for some practical examples). Although initially applied to *T-P* phase diagrams, the method is general and can be applied to *T-X* diagrams, or activity–activity diagrams, or any other diagram involving two intensive variables. We shall use *T-P* diagrams for our examples.

Suppose we begin with a *C* component system. When there are $C + 2$ phases (ϕ) present at equilibrium, $F = C - \phi + 2 = 0$. This is an invariant situation in which all intensive variables, including *T* and *P*, are fixed, and is represented by an invariant point on a *T-P* phase diagram. If one phase were absent, we would have a univariant situation, represented by a curve on a *T-P* diagram. Because there are $C + 2$ possible phases at the invariant point, any one may be absent, and it follows that there must be $C + 2$ possible univariant curves emanating from the invariant point, each with a different phase absent.

For example, Figure 15 shows the one-component Al_2SiO_5 system (if we ignore SiO_2, H_2O, and the formation of pyrophyllite). All three polymorphs $(C + 2)$ can coexist at the invariant point. From that point, three $(C + 2)$ univariant curves emanate, each missing one phase $(C + 1$ phases are present$)$. The phase that is *absent* serves to identify the reaction represented by any univariant curve. Thus the Ky-And reaction is the Sil-absent reaction, etc. The absent phase (in parentheses) may thus be used as a unique label for each curve, as has been done in Figure 15. The short dashed lines in Figure 15 are **metastable extensions** of each stable curve, where it extends beyond the invariant point into the field in which the absent phase is stable.

Systems with more than $C + 2$ possible phases are called **multisystems** and contain more than one invariant point.

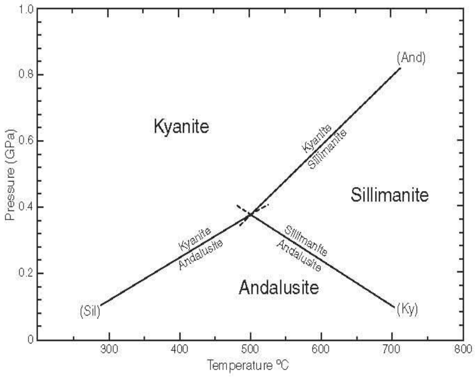

FIGURE 15 An Al_2SiO_5 *T-P* phase diagram.

A situation for the general case of a one-component system with four possible phases (*A*, *B*, *D*, and *E*) is illustrated in Figure 16. Because there can be only $C + 2 = 3$ phases at an invariant point, and there are four phases in the system, we can readily deduce that four invariant points are possible, each of which is missing one phase. The four invariant points have been labeled in Figure 16 with the absent phase in square brackets. From each invariant point there emanate three univariant curves, each with $C + 1 = 2$ phases at equilibrium along the curve. Univariant curves have been labeled in Figure 16, with the absent phase in parentheses. For example, invariant point [*D*] in the upper right of the diagram has univariant curves (*A*), (*B*), and (*E*) emanating from it. Curve (*E*), for example, as it emanates from invariant point [*D*] must have both phase *E* and phase *D* absent because it is the *E*-absent curve emanating from the *D*-absent invariant point. It is thus the curve that represents $A = B$ equilibrium, which separates the *A* and *B* stability fields. (Divariant fields in one-component systems have one phase.) Notice that this same univariant reaction curve is the *D*-absent curve emanating from the *E*-absent invariant point. All four invariant points operate in a similar way, and the entire diagram is internally consistent, in that it separates the *P-T* area into four divariant stability fields, each with $C = 1$ phase (labeled without brackets or parentheses).

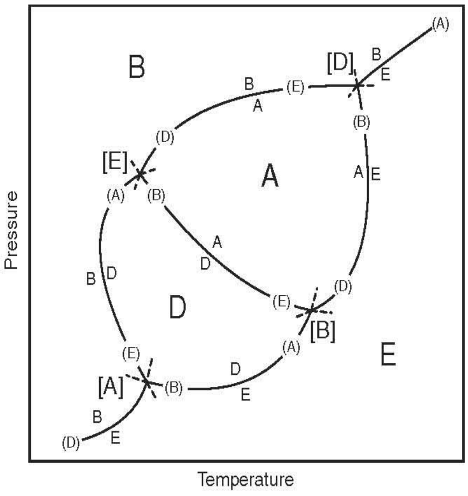

FIGURE 16 Schematic one-component *T-P* phase diagram, showing the topology of a four-phase multisystem in which all invariant points are stable. Because only three phases ($C + 2$) coexist at an invariant point, a complete system should have four invariant points, each with one phase absent. Phases absent at invariant points are in square brackets, phases absent for univariant reactions are in parentheses.

Figure 16 represents a situation in which all four possible invariant points are stable at reasonable pressures and temperatures. It can be seen that such a diagram requires substantial curvature of many reaction curves in order to satisfy the Schreinemakers topologies. In most phase diagrams, such as the SiO_2 diagram, one or more of the possible invariant points may not be stable because they occur at unrealistically high or low *P-T* conditions, or they are intrinsically metastable (the intersection of metastable extensions, not of stable curves). Figure 17 illustrates the concept with a portion of the SiO_2 phase diagram, showing the situation for a four-phase, one-component subset of the system. Only two of the possible invariant points, [Liq] and [Trd], are present. The [β-Qtz] invariant point occurs at negative pressure, and the [Crs] invariant point is not stable because it occurs at the intersection of metastable extensions, not of stable univariant curves. This diagram also satisfies all the Schreinemakers criteria.

The And-Sil-Ky invariant point is the pyrophyllite-absent invariant point [similar to (*B*) in Figure 16], and the Prl-And-Ky invariant point is the Sil-absent invariant point [similar to (*E*) in Figure 16]. The other possible invariant points are not sta-ble. The And-absent invariant point, for example, requires the Ky-Sil reaction to curve back and intersect the Prl-Ky curve, which does not happen at any realistic pressure.

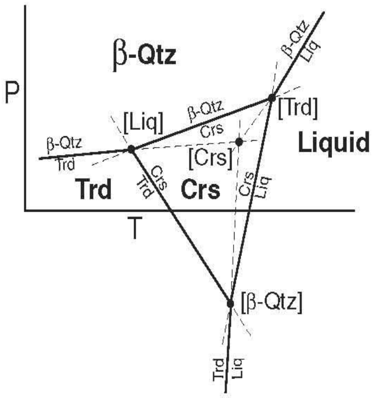

FIGURE 17 A portion of the *P-T* phase diagram for SiO_2, showing two stable invariant points [Trd] and [Liq] and two metastable ones. [β-Qtz] occurs at negative pressure, and [Crs] is truly metastable in that it is the intersection of metastable extensions. From Spear (1993).

Some important geometric rules for dealing with systems of C components that stem from both the phase rule and the method of Schreinemakers include:

1. When $\phi = C + 2$, an invariant point results.
2. $C + 2$ univariant curves must emanate from each invariant point.
3. If two reactions have fewer than C phases in common, they cross in an **indifferent** fashion: they are independent of each other and do not require an invariant point at the intersection. For example, the high-quartz/low-quartz reaction may cross the And-Sil reaction, and neither is affected by the other.
4. If, on the other hand, two intersecting univariant reactions have C phases in common, their intersection cannot be indifferent, and the intersection generates an invariant point, plus other univariant curves emanating from it, as described in rules 1 and 2 above. This is so because each univariant curve must have $C + 1$ phases at equilibrium, and one of the phases cannot be the same for each intersecting curve (otherwise, they would be the same curve). Thus $C + 2$ phases coexist at the intersection of the curves, and this implies an invariant situation.
5. Consider a univariant reaction such as $D + E = F$ in a two-component system in Figure 18a. The reaction is univariant in a two-C system because it has $C + 1 = 3$ phases at equilibrium. If it intersects another univariant reaction curve at an invariant point, *the D-absent and E-absent curves must both occur on the side of the initial reaction opposite to the field in which D and E are stable* (see Figure 18b for an example using the D-absent reaction). Similarly, the F-absent reaction must lie on the opposite side of the initial reaction, the side opposite the field in which F is stable. *The metastable extensions of each of these reactions will thus lie on the side of the first reaction in which the absent-phase is stable.* For example, the metastable extension of the D-absent reaction is on the side of the first reaction in which phase *D is* stable. This is a fundamental axiom of the Schreinemakers approach and must apply to all reactions that meet at an invariant point.
6. It follows from rule 5 that if two reactions that meet at an invariant point are known and can be located and oriented fairly accurately on a phase diagram, the full topology of the invariant point can be deduced.
7. It also follows from rule 5 that any divariant field cannot occupy a sector >180° about any invariant point. Otherwise, the metastable extension would extend into the field in which the phase is unstable.

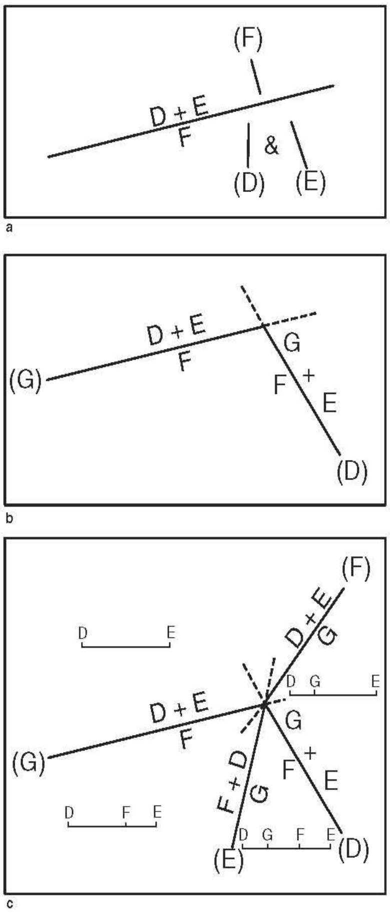

FIGURE 18 **(a)** Hypothetical reaction $D + E = F$ in a two-component phase diagram. Note that the D-absent and E-absent curves must both lie on the side of the initial univariant curve opposite the field in which $D + E$ is stable. Likewise, the F-absent curve must lie on the side opposite to the field in which F is stable. **(b)** A second hypothetical univariant curve (D-absent) is added. **(c)** The complete topology of the invariant point can then be derived from the two initial reactions in **(b)**. The chemographics may then be added to each divariant field.

Figure 18 illustrates the Schreinemakers rules for a two-component, four-phase system. Suppose we begin with the reaction $D + E = F$ (Figure 18a) and add another well-constrained reaction, such as $F = G + E$ (Figure 18b). Because these two reactions have C phases in common (E and F), their intersection requires an invariant point with $C + 2 = 4$ phases in equilibrium and $C + 2 = 4$ reactions emanating from it. The initial reaction must be G-absent, the second reaction must be D-absent, and we can apply rule 5 above to both reactions simultaneously. This implies that reaction (E) must be on the lower side of reaction (G) *and* on the left side of reaction (D) (Figure 18c). Reaction (F) must be on the upper side of reaction (G) *and* on the right side of reaction (D). We can then determine what phases occur on which side of each of the remaining two reactions, so that rule 5 applies to all four reactions simultaneously. From that, we have the full topology of the invariant point and the reactions in Figure 18c (rule 6). Affirm for yourself that rule 5 applies to all the reactions, and the metastable extension of any reaction (x-absent) is on the side of the other three reactions where x is stable. Note also that all two-phase divariant assemblages occupy sectors <180° about the invariant point (rule 7). The binary chemographic compatibility diagrams have also been added to each divariant field in Figure 18c such that each field has a unique compatibility diagram. As an exercise, demonstrate to your satisfaction that each reaction causes changes in the chemographic topologies on either side of it in a fashion consistent with the geometries discussed in the previous section.

Note that rules 5 and 7 also apply to Figure 15 and any other phase diagram. In Figure 15, the andalusite-absent reaction is on the side of the sillimanite-absent reaction that is opposite to the andalusite field, and the metastable extension is within the andalusite field, etc. Similarly, crossing the pyrophyllite reaction with the And-Ky reaction is *not* an indifferent crossing, and thus the kink in the curve as it changes from And + Qtz + H_2O = Prl to Ky + Qtz + H_2O = Prl is required by rules 5 and 7 above.

The geometric approach of Schreinemakers is useful and is used in conjunction with experimental and theoretical data to develop more comprehensive phase diagrams and petrogenetic grids. Although numerous univariant equilibrium curves have been studied experimentally, rarely has every curve that emanates from any given invariant point been located accurately. Just as in Figure 18, the method of Schreinemakers permits investigators to infer the general location of the other reactions about an invariant point if two are known from experiments. If some thermodynamic data are available on the phases involved in the reactions, we could calculate the slope from the Clapeyron equation and further refine the geometries. Even a simple knowledge of relative molar volumes of the minerals and the characteristic shape of devolatilization reaction curves is useful in refining the arrangement of univariant curves about an invariant point.

The geometric method has three shortcomings that cannot be resolved without good experimental and/or thermodynamic data. First, the *location* of any invariant point cannot be determined using the Schreinemakers method; only the topology can be determined. Second, the exact slope or location of any univariant reaction curve likewise cannot be known. Finally, for any topology such as that in Figure 18c, an alternative enantiomorphic topology (a mirror image) is also compatible with the Schreinemakers rules. Which choice is real cannot be known from the geometric approach alone. All of these shortcomings can be resolved if sufficient physical–thermodynamic data are available.

There remains one final point to mention. The ideal topologies, such as those illustrated in Figures 16 and 18, hold only in the general case of non-degenerate systems. **Degenerate** systems are those in which the composition of some of the phases is related in a particular way. For example, in a system of two or more components, the composition of some phases may be identical. This is the case in a three-component Al_2O_3-SiO_2-H_2O system, and three of the phases all have the composition Al_2SiO_5. Thus the Prl-absent curve that emanates from the five-phase Prl-Qtz-And-Ky-H_2O invariant point is also the *Qtz*-absent and the H_2O-absent curve as well. Thus there are $C - 1$, and not $C + 2$, curves emanating from the invariant point because of the degeneracy. Another type of degeneracy results when three phases plot along a single line in a $C > 3$ system, or when four phases are coplanar in a $C > 4$ system, etc. In all degenerate cases, there may be fewer than $C + 2$ univariant curves emanating from an invariant point.

11 PETROGENETIC GRIDS

A **petrogenetic grid** is a *P-T-X* (or *P-T*, *T-X*, *P-X*) phase diagram for a particular chemical system or bulk composition that illustrates several important reactions for that system. When Bowen (1940) proposed the term, he had the vision of a complete characterization of all divariant mineral assemblages in nature but realized that the magnitude of undertaking the necessary experiments was a huge task that would not be finished for a long time. Modern petrogenetic grids are thus only partially complete (although advances in thermodynamic databases and computer programs allow us to create increasingly more accurate multisystems). Choosing an appropriate chemical system and the reactions to use requires a combination of good lab work on a suite of rocks (and/or good theoretical data) and good judgment. When making the choice, we face the same problem as with modeling igneous crystallization and melting behavior. Simple chemical systems generate simple phase diagrams that may allow us to understand some fundamental features, but most are drastic oversimplifications of natural rock systems. Complex chemical systems may be more realistic, but the petrogenetic grid may become so cluttered that it becomes difficult to recognize the reactions that are most important in the petrogenesis of some rock types.

A petrogenetic grid may be simple, or it may be a full multisystem of five to eight components containing dozens of invariant points and a hundred or more reactions. Most good petrogenetic grids are a judicious compromise of three to six components and a selection of the most definitive reactions and invariant points. These reactions provide the best quantitative *P-T-X* constraints on the conditions of metamorphism that produce the common mineral assemblages of a class of metamorphic rocks. Because only selected reactions are included, many grids do not have the complete Schreinemakers topologies for all invariant points.

Figure 19 is an example of a petrogenetic grid for metamorphosed mafic rocks. It illustrates many of the important reactions that govern the development of mafic mineral assemblages from the zeolite to the granulite facies, as well as the blueschist and eclogite facies at higher pressures. For a more complete version, see Chapter 9 of Bücher and Frey (2002), and for higher pressures see Guiraud et al. (1990), or Poli and Schmidt (2002). The grid illustrates several important reactions, including those that govern the transitions from one facies to the next. As you study the diagram, you may notice the reactions that govern the development of zeolites, prehnite and pumpellyite, the formation of glaucophane or the decomposition of plagioclase at high pressure, the development of epidote and actinolite of the greenschist facies, hornblende and plagioclase of the amphibolite facies, and the dehydration of hornblende to form pyroxene-bearing granulite facies assemblages. Notice

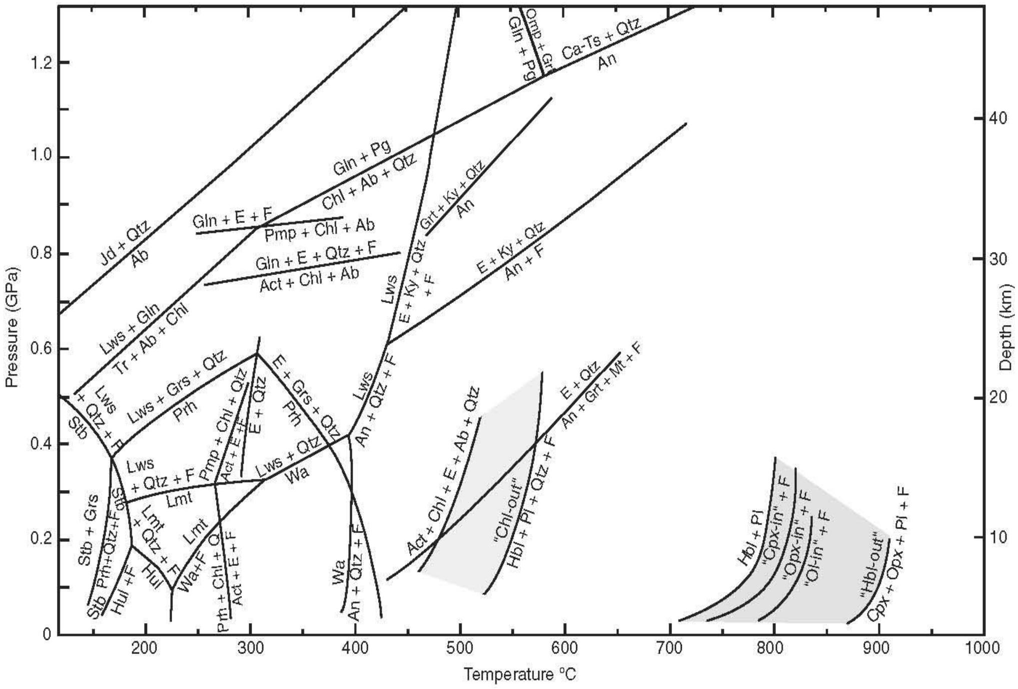

FIGURE 19 Simplified petrogenetic grid for metamorphosed mafic rocks, showing the location of several determined univariant reactions in the CaO-MgO-Al_2O_3-SiO_2-H_2O-(Na_2O) system ("C(N)MASH"). Mineral abbreviations are listed in the inside cover (*F* = aqueous fluid, *E* = an epidote mineral: epidote, zoisite, or clinozoisite). Important continuous reactions are shaded (although most reactions are continuous with respect to Fe-Mg, Ca-Na, or some other components). Data from Liou (1970, 1971a, b, c), Liou et al. (1974, 1985, 1987), Cho et al. (1987), Maruyama and Liou (1988), Maruyama et al. (1986), Newton and Smith (1967), Newton (1986), Newton and Kennedy (1963), Evans (1990), Massone (1989), Spear (1981), and Bucher and Frey (2002).

also that many of these important reaction isograds span a limited *P-T* range and would be intersected by only certain facies series or *P-T-t* paths. Other reaction isograds cross (indifferently in many cases). For example, the epidote → anorthite reaction in the center of the grid below 0.6 GPa has a shallower slope than does the actinolite → hornblende reaction. Because fewer than *C* phases are in common between the two reactions, the crossing is indifferent, and an invariant point does not result. This crossing explains why the albite → plagioclase transition occurs before actinolite → hornblende for low-pressure metamorphism, and the opposite is true for higher *P-T-t* paths.

12 REACTION MECHANISMS

The discussion of metamorphic reactions in the preceding sections of this chapter has dealt with relatively simple balanced reactions and the location of the equilibrium reaction boundaries on phase diagrams. Little attention has been paid to the actual *mechanism* by which a reaction might take place in the rocks themselves. Dugald Carmichael (1969) pointed out that the textures seen in thin section may not coincide with the reaction that may be deduced by simply comparing the reactant and product mineral assemblages. Although there is certainly a gradual reduction in reactant minerals across any reaction isograd, and this is compensated by growth of the product assemblage, the products in many cases do not grow in direct contact with the reactants. Rather, the products and reactants are found in different domains of a thin section, separated by "inert" minerals that are stable on both sides of the reaction. In other words, the most obvious and simple balanced reaction may not reflect the true mechanism by which the overall reaction was accomplished.

For example, the simple reaction of kyanite → sillimanite at the sillimanite isograd in pelites rarely results in the sillimanite directly replacing the kyanite as pseudomorphs. Rather, small sillimanite crystals (commonly as fibrolite) occur embedded in muscovite, biotite, or quartz. A common texture is illustrated in Figure 20a, in which several blebs of kyanite and quartz occur in a larger host muscovite crystal. The kyanite and quartz grains appear to be remnants of larger crystals, as neighboring grains of each mineral type are in optical continuity (they go extinct in unison), and kyanite cleavages have the same orientation. Fine sillimanite crystals appear to have grown nearby in the muscovite.

Carmichael (1969) noted that such a texture does not support the simple Ky → Sil reaction occurring as such and used the textures to infer an alternative mechanism involving dissolution and transport on a localized scale. Assuming that

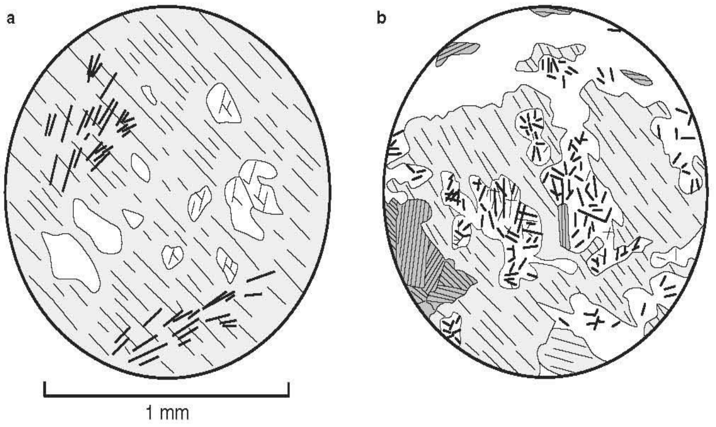

FIGURE 20 **(a)** Sketch from a photomicrograph, showing small crystals of kyanite (with cleavages) and quartz in a larger muscovite grain (shaded with NW–SE cleavages). Small crystals of fibrolitic sillimanite also occur in the muscovite. Glen Cova, Scotland. **(b)** Sillimanite needles in quartz embaying muscovite. Darker crystals are biotite. Donegal, Ireland. After Carmichael (1969). Copyright © with permission from Springer-Verlag.

Al_2O_3 (a notably insoluble component in most pelites) is conserved, he proposed that kyanite broke down by the reaction:

$$\underset{\text{Ky}}{3\,\text{Al}_2\text{SiO}_5} + \underset{\text{Qtz}}{3\,\text{SiO}_2} + 2\,\text{K}^+ + 3\,\text{H}_2\text{O} \rightarrow \underset{\text{Ms}}{2\,\text{KAl}_2\text{Si}_3\text{AlO}_{10}(\text{OH})_2} + 2\text{H}^+ \tag{18}$$

Rims of muscovite appear to grow at the expense of Ky and Qtz, and they gradually encroach on both as the reaction advances, leaving isolated patches of the reactants, as observed in Figure 20a. Such a reaction consumes K^+ and H_2O, and releases H^+, all of which involve exchange of ions between minerals and a fluid phase. For the reaction to proceed, there must be a source of K^+ and a receptor for H^+. This may involve an external source (such as a nearby granite) and sink, but other local solution–precipitation reactions may occur in the same rock to fulfill these roles, alleviating the need for an external reservoir. Carmichael (1969) noted another common texture in many pelites in which needles of sillimanite occur in quartz embayments into ragged muscovite crystals (Figure 20b). A reaction capable of producing this texture that conserves Al_2O_3 is:

$$\underset{\text{Ms}}{2\,\text{KAl}_2\text{Si}_3\text{AlO}_{10}(\text{OH})_2} + 2\,\text{H}^+ \rightarrow \underset{\text{Sil}}{3\,\text{Al}_2\text{SiO}_5} + \underset{\text{Qtz}}{3\,\text{SiO}_2} + 2\,\text{K}^+ + 3\,\text{H}_2\text{O} \tag{19}$$

This reaction consumes muscovite and produces sillimanite and quartz, which explains the embayed muscovite and quartz–sillimanite filling the embayments. If Reactions (18) and (19) occur simultaneously, then each serves as both source and sink for the fluid and solute species of the other, muscovite is conserved, and the *net reaction* is Ky → Sil.

Figure 21 shows that the overall reaction can be considered the sum of two local reactions that operate similarly to the "half-cell" reactions used to demonstrate the electromotive series in chemistry labs.

Carmichael (1969) proposed a number of other such "half-cell" type reactions that may substitute for isograd reactions and provide better explanations for the observed textures. Any isograd may have a number of alternative combined reactions that involve ionic species that contribute to the net isograd reaction. An alternative mechanism for the Ky → Sil isograd that explains the very common occurrence in some pelites of sillimanite (or fibrolite) in biotite, rather than replacing kyanite, consists of three separate exchange subreactions. The first is Reaction (18), and the other two are:

$$\underset{\text{Bt}}{\text{K(Mg, Fe)}_3\text{Si}_3\text{AlO}_{10}(\text{OH})_2} + \text{Na}^+ + 6\,\text{H}^+ \rightarrow \underset{\text{Ab}}{\text{NaAlSi}_3\text{O}_8} + \text{K}^+ + 3(\text{Mg, Fe})^{2+} + 4\,\text{H}_2\text{O} \tag{20}$$

$$\underset{\text{Ms}}{2\,\text{KAl}_2\text{Si}_3\text{AlO}_{10}(\text{OH})_2} + \underset{\text{Ab}}{\text{NaAlSi}_3\text{O}_8} + 3\,(\text{Mg, Fe})^{2+} + 4\,\text{H}_2\text{O} \rightarrow \underset{\text{Bt}}{\text{K(Mg, Fe)}_3\text{Si}_3\text{AlO}_{10}(\text{OH})_2} + \underset{\text{Sil}}{3\,\text{Al}_2\text{SiO}_5} + \underset{\text{Qtz}}{3\,\text{SiO}_2} + \text{K}^+ + \text{Na}^+ + 4\,\text{H}^+ \tag{21}$$

Notice that Reaction (21) produces biotite and sillimanite, which are commonly found in association, while consuming albite. Reaction (20) replaces the albite, which produces biotite crystals embayed by plagioclase. Reactions

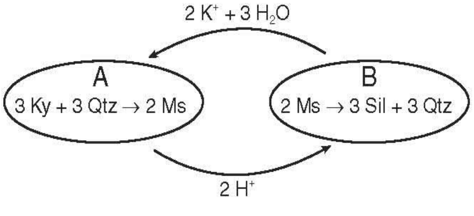

FIGURE 21 A possible mechanism by which the Ky → Sil reaction can be accomplished while producing the textures illustrated in Figure 20a and b. The exchange of ions shown between the two local zones is required if the reactions are to occur. After Carmichael (1969). Copyright © with permission from Springer-Verlag.

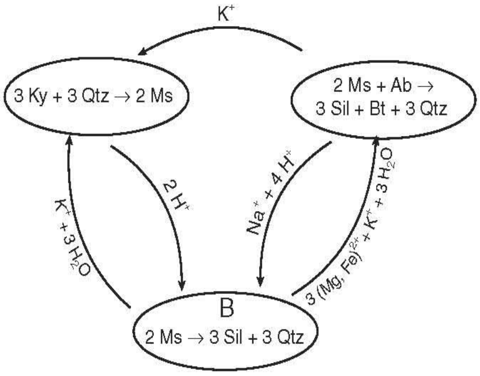

FIGURE 22 An alternative mechanism by which the Ky → Sil reaction can be accomplished while producing sillimanite needles associated with biotite, whereas plagioclase occupies embayments in the biotite. The exchange of ions shown between the two local zones is required if the reactions are to occur. After Carmichael (1969). Copyright © with permission from Springer-Verlag.

(18), (20), and (21) can be combined to eliminate the fluid and solute species and produce the Ky → Sil net reaction. Figure 22 illustrates the overall process and local exchanges required by such a net reaction. This alternative to Figure 21 appears to occur in rocks where sillimanite is associated with biotite instead of with muscovite.

Two requirements must be met if the coupled exchange reactions are to work. First, there must be sufficient fluid and ionic mobility for the exchange to occur between the two zones in the rock. Mass transfer for such reactions may be on the scale of millimeters to (rarely) several meters. Second, the Ky → Sil univariant reaction curve in Figure 15 must be overstepped, so that sillimanite, rather than kyanite, is produced by Reaction (19). Thus the net reaction of Ky → Sil is still a proper *overall* reaction for the sillimanite isograd. Although the mechanism and textures differ, the isograd and the *P-T* stability conditions that it represents are still valid. Thus we can still treat the reaction equilibrium–thermodynamically as Ky → Sil.

Carmichael's (1969) proposal suggests that reactions involving dissolved species may be much more common than we previously thought, and it also explains why fluids can catalyze solid–solid reactions such as polymorphic transformations, which do not appear, at first glance, to involve fluids at all. Several investigators have carried this idea beyond Carmichael's initial work. Fisher (1973, 1977), Frantz and Mao (1976), Loomis (1976), Foster (1981, 1983), Likhanov and Reverdatto (2002), and others have developed methods (most based on non-equilibrium irreversible thermodynamics) to model mineral dissolution and diffusion along chemical potential gradients to add a quantitative aspect to such reaction mechanisms. In his summary, Putnis (2002) suggested that mineral replacement reactions (including isochemical replacement and pseudomorphs) occur *primarily* by dissolution–reprecipitation processes involving exchange of dissolved species, typically along a sharp replacement front. Ferry (2000) noted that pseudomorphs are much more common results of retrograde processes than of prograde metamorphism. He noted that prograde reactions are typically devolatilization reactions with positive dP/dT slopes and positive ΔV of reaction and he suggested that the added volume of the mineral(s) produced when a mineral breaks down exerts a local "force of crystallization" at the breakdown surface. The local pressure rise at the mineral surface would increase strain and inhibit a pseudomorphing process. The products therefore develop better at some site away from the expanding mineral breakdown surface, presumably by a dissolution–migration–precipitation process such as Carmichael and others have described. Fluid release during prograde devolatilization should also greatly enhance such processes. Retrograde reactions, on the other hand, involve a negative ΔV and, according to this theory, would make the interface a more favorable site for the retrograde reaction, which, in combination with reduced fluid availability, makes a pseudomorph more likely.

Summary

Changes in the mineral assemblages in rocks must involve reactions in which one or more reactant minerals are consumed and other product minerals are produced. Reactions can be of various types. Polymorphic transformations involve the change of one mineral to another of the same composition. Exsolution reactions involve the unmixing of solid solution minerals accompanying cooling or, less commonly, decompression. Solid–solid net transfer reactions are a common type of reaction that involves multiple solids, requiring that matter must migrate from reactant minerals as they break down to the sites of product mineral growth. When solid solution is limited, these reactions are discontinuous (they occur abruptly at a single metamorphic grade). These three types of reactions are relatively easy to constrain, as they are dependent only on temperature and pressure (and the attainment of equilibrium, of course).

Devolatilization reactions involve the breakdown of one or more volatile-bearing minerals and release of a volatile species (typically H_2O or CO_2, but any volatile may be possible). Such reactions depend on the partial pressures of the volatiles in the system as well as on temperature and pressure. Such reactions occur at the maximum grade possible when the partial pressure of the volatile species released equals the total pressure. When $P_{fluid} < P_{lithostatic}$ or the fluid is diluted with another volatile species, the reaction occurs at lower grades. If a rock system is open to the passage of fluids, the fluid composition remains constant, and devolatilization reactions occur at a single grade. If fluid motion is limited, a devolatilization reaction will span a range of grades and buffer the fluid composition across the range.

Continuous reactions involve solid solutions and take place over a range of temperatures (grades). The grade at which a product mineral first appears (an isograd) with such a reaction depends on the bulk composition. The reaction spans a range of grades as the reactants are gradually consumed and products generated, and the composition of each varies systematically over the range. Ion exchange reactions involve the reciprocal exchange of components (most commonly Fe versus Mg) between two or more minerals (without changing the modal amounts of any). Oxidation/reduction (redox) reactions involve changes in the ionic charge of atoms or complexes (e.g., Fe^{2+} to Fe^{3+}), typically involving a compensating change in the charge of oxygen. Many reactions involve the release, migration, and capture of dissolved species in order to maintain equilibrium between the reacting phases.

Many reactions can readily be visualized and understood by some simple geometric patterns of phase locations in appropriately developed chemographic diagrams. As a general rule, combining two or more phases yields a bulk composition within the line or polygon bounded by those phases. If two such combinations, each consisting of unique phases, can be combined to yield a point of identical X_{bulk}, the two groups are compositionally equivalent and may potentially be related by a balanced reaction. These geometric changes, involving the loss or introduction of a phase or simply rearranging the tie-lines that connect coexisting phases, are what relate composition paragenesis (compatibility) diagrams from one facies or zone to the next as a reaction takes place. A petrogenetic grid is a *P-T-X* phase diagram for a particular chemical system that illustrates several important reactions for that system. Geometric principles may also be applied to phase diagrams and petrogenetic grids: the method of Schreinemakers is a formalized geometric procedure for organizing the topology of reaction curves about invariant points on such diagrams.

Key Terms

Isograds: mineral-in, mineral-out
Polymorphic transformation reactions
Exsolution reactions
Solid–solid net transfer reactions
Devolatilization reactions
Partial pressure (p_{H_2O}, p_{CO_2})
T-X_{fluid} phase diagram
Open-system and closed system volatile behavior
Buffer
Continuous reaction
Pseudosection
Ion-exchange reaction
Blocking or closure temperature
Oxidation/reduction (redox) reaction
Oxygen buffer
Dissolved species and hydrolysis
Topology
Tie-line flip
Schreinemakers method
Metastable extension
Multisystem
Indifferent reaction intersection
Petrogenetic grid

Review Questions and Problems

Review Questions and Problems are located on the author's web page at the following address: **http://www.prenhall.com/winter**

Important "First Principle" Concepts

- Because the temperature of a devolatilization reaction depends on the partial pressure of the volatile species involved, one should take great care to constrain the fluid composition, if at all possible, before using a devolatilization reaction to indicate metamorphic grade.
- The metamorphic grade at which a continuous reaction occurs depends on the composition of the phases, which, in turn, is dependent upon X_{bulk}.
- Continuous reactions span an interval of grade, across which the reactants are progressively consumed, products are generated, and the compositions of each vary systematically.
- Reactions involve changes in topology of compatibility diagrams: loss or introduction of a phase or rearranging of tie-lines that connect coexisting phases. Therefore, each facies or zone may be represented by a compatibility diagram that differs from the neighboring zone by a reaction and a very specific geometric change in topology that is related to that reaction.

Suggested Further Readings

Bücher, K., and M. Frey. (2002). *Petrogenesis of Metamorphic Rocks*. Springer-Verlag. Berlin. Chapter 3.

Carmichael, D. M. (1969). On the mechanism of prograde metamorphic reactions in quartz-bearing pelitic rocks. *Contrib. Mineral. Petrol.*, **20**, 244–267.

Kretz, R. (1994). *Metamorphic Crystallization*. John Wiley & Sons. New York. Chapter 3.

Zen, E-an. (1966). Construction of pressure–temperature diagrams for multi-component systems after the method of Schreinemakers—A geometric approach. *U.S. Geol. Survey Bulletin* **1225**.